quire clarification about how the alterations in the concentrations of these miRNAs in maternal plasma affect specific gene expression in some maternal tissues.

Author Contributions: *All authors confirmed they have contributed to the intellectual content of this paper and have met the following 3 requirements: (a) significant contributions to the conception and design, acquisition of data, or analysis and interpretation of data; (b) drafting or revising the article for intellectual content; and (c) final approval of the published article.*

Authors' Disclosures of Potential Conflicts of Interest: *Upon manuscript submission, all authors completed the Disclosures of Potential Conflict of Interest form. Potential conflicts of interest:*

Employment or Leadership: None declared.
Consultant or Advisory Role: None declared.
Stock Ownership: None declared.
Honoraria: None declared.
Research Funding: K. Miura, Grant-in-Aid for Young Scientists (B) (no. 21791567) from the Ministry of Education, Sports, Culture, Science and Technology of Japan; Seed Grant (no. J089500122) from the Japan Science and Technology Agency (JST); grants from the Naito Foundation; and a grant for Child Health and Development (no. 20C-1) from the Ministry of Health, Labour and Welfare, Japan; K. Yoshiura, Grants-in-Aid for Scientific Research from the Ministry of Health, Labour and Welfare, Japan.
Expert Testimony: None declared.

Role of Sponsor: The funding organizations played no role in the design of study, choice of enrolled patients, review and interpretation of data, or preparation or approval of manuscript.

References

1. Lee RC, Feinbaum RL, Ambros V. The *C. elegans* heterochronic gene lin-4 encodes small RNAs with antisense complementarity to lin-14. Cell 1993;75:843–54.
2. Mendell JT. MicroRNAs: critical regulators of development, cellular physiology and malignancy. Cell Cycle 2005;4:1179–84.
3. Plasterk RH. Micro RNAs in animal development. Cell 2006;124:877–81.
4. Chiu RW, Lui WB, Cheung MC, Kumta N, Farina A, Banzola I, et al. Time profile of appearance and disappearance of circulating placenta-derived mRNA in maternal plasma. Clin Chem 2006;52:313–6.
5. Purwosunu Y, Sekizawa A, Farina A, Wibowo N, Okazaki S, Nakamura M, et al. Cell-free mRNA concentrations of CRH, PLAC1, and selectin-P are increased in the plasma of pregnant women with preeclampsia. Prenat Diagn 2007;27:772–7.
6. Lo YM, Chiu RW. Prenatal diagnosis: progress through plasma nucleic acids. Nat Rev Genet 2007;8:71–7.
7. Maron JL, Bianchi DW. Prenatal diagnosis using cell-free nucleic acids in maternal body fluids: a decade of progress. Am J Med Genet C Semin Med Genet 2007;145:5–17.
8. Miura K, Miura S, Yamasaki K, Yoshida A, Yoshiura K, Nakayama D, et al. Increased level of cell-free placental mRNA in a subgroup of placenta previa that needs hysterectomy. Prenat Diagn 2008;28:805–9.
9. Chim SS, Shing TK, Hung EC, Leung TY, Lau TK, Chiu RW, Lo YM. Detection and characterization of placental microRNAs in maternal plasma. Clin Chem 2008;54:482–90.
10. Luo SS, Ishibashi O, Ishikawa G, Ishikawa T, Katayama A, et al. Human villous trophoblasts express and secrete placenta-specific microRNAs into maternal circulation via exosomes. Biol Reprod 2009;81:717–29.
11. Chiu RW, Poon LL, Lau TK, Leung TN, Wong EM, Lo YM. Effects of blood-processing protocols on fetal and total DNA quantification in maternal plasma. Clin Chem 2001;47:1607–13.
12. Bentwich I, Avniel A, Karov Y, Aharonov R, Gilad S, Barad O, et al. Identification of hundreds of conserved and nonconserved human microRNAs. Nat Genet 2005;37:766–70.
13. Tsai KW, Kao HW, Chen HC, Chen SJ, Lin WC. Epigenetic control of the expression of a primate-specific microRNA cluster in human cancer cells. Epigenetics 2009;4:587–92.
14. Seitz H, Royo H, Bortolin ML, Lin SP, Ferguson-Smith AC, Cavaillé J. A large imprinted microRNA gene cluster at the mouse Dlk1-Gtl2 domain. Genome Res 2004;14:1741–8.
15. Royo H, Bortolin ML, Seitz H, Cavaillé J. Small non-coding RNAs and genomic imprinting. Cytogenet Genome Res 2006;113:99–108.

Previously published online at
DOI: 10.1373/clinchem.2010.147660

ANTICANCER RESEARCH *30*: 5189-5194 (2010)

Association between Breast Cancer Risk and the Wild-type Allele of Human ABC Transporter *ABCC11*

IKUKO OTA[1,2], AKI SAKURAI[3], YU TOYODA[3], SATOSHI MORITA[4], TAKESHI SASAKI[5], TAKASHI CHISHIMA[1], MINORU YAMAKADO[6], YUKI KAWAI[7], TAKEFUMI ISHIDAO[7], ALEXANDER LEZHAVA[8], KOH-ICHIRO YOSHIURA[9], SHINJI TOGO[1], YOSHIHIDE HAYASHIZAKI[8], TAKASHI ISHIKAWA[2], TOSHIHISA ISHIKAWA[3,8], ITARU ENDO[1] and HIROSHI SHIMADA[1]

[1]*Department of Gastroenterological Surgery, Yokohama City University Graduate School of Medicine and Departments of* [2]*Breast and Thyroid Surgery,* [4]*Biostatistics and Epidemiology and* [5]*Pathology, Yokohama City University Medical Center, Yokohama, Japan;*
[3]*Department of Biomolecular Engineering, Graduate School of Bioscience and Biotechnology, Tokyo Institute of Technology, Yokohama, Japan;*
[6]*Center for Multiphasic Health Testing and Services, Mitsui Memorial Hospital, Tokyo, Japan;*
[7]*K.K. DNAFORM, Yokohama, Japan;*
[8]*Omics Science Centre, RIKEN Yokohama Institute, Yokohama, Japan;*
[9]*Department of Human Genetics, Nagasaki University Graduate School of Biomedical Sciences, Nagasaki, Japan*

Abstract. *Background: International mortality and frequency rates for breast cancer have been associated with the wet type of human earwax. It was recently found that earwax type is determined by a single nucleotide polymorphism (SNP), 538G>A (Gly180Arg), in ABCC11. The G allele determines the wet type of earwax as a Mendelian trait with a dominant phenotype. The present study examined the association between the frequency rate of breast cancer and the frequency of the G allele of ABCC11. Patients and Methods: Using blood samples from patients with invasive breast cancer (n=270) and control volunteers (n=273), the 538G>A SNP in ABCC11 was genotyped using the SmartAmp method. Results: The frequency of the G allele in breast cancer patients was higher than that in healthy controls. The odds ratio for the genotypes (G/G+G/A) to develop breast cancer was estimated to be 1.63 (p-value=0.026), suggesting that the G allele in ABCC11 is associated with breast cancer risk. Conclusion: This study showed that Japanese women with wet earwax have a higher relative risk of developing breast cancer than those with dry earwax. The ABCC11 SNPs that determine these phenotypes should be further investigated in order to obtain insights into the mechanisms by which breast cancer develops and progresses.*

Correspondence to: Toshihisa Ishikawa, Ph.D., Omics Science Centre, RIKEN Yokohama Institute, 1-7-22 Suehiro-cho, Tsurumi-ku, Yokohama 230-0045, Japan. Tel: +81 455039222; Fax: +81 455039216, e-mail: toshi-i@gsc.riken.jp

Key Words: Apocrine gland, axillary osmidrosis, earwax, mammary gland, SNP, ABC transporter *ABCC11*, breast cancer risk.

Breast cancer is the most common cancer among women in the industrialised world, where it accounts for 22% of all cancers in women. There has been increased interest in the genetic predisposition for many common cancer types, including breast cancer (1). In 1971, Nicholas L. Petrakis first reported that international mortality and frequency rates for breast cancer appeared to be associated with the frequency of the allele for wet-type earwax (2). Caucasian and African-American women in the USA as well as German women exhibited approximately four-fold higher rates of breast cancer mortality than Japanese and Taiwanese women (2). Nevertheless, the phenotypic association of the wet type of earwax with breast cancer has remained controversial (2, 3).

Recent studies (4, 5) have provided evidence that the type of earwax is determined by one single nucleotide polymorphism (SNP), 538G>A (Gly180Arg), in the ATP-binding cassette (ABC) transporter *ABCC11* located on human chromosome 16q12.1 (6). The G/G and G/A genotypes correspond to the wet type of earwax, whereas A/A corresponds to the dry type (5). Wide ethnic differences have been observed in the frequencies of those alleles (4, 7). Among worldwide populations, the 'G' (wild-type) allelic frequency shows striking downward geographical gradient distributions from Africa to Far East Asia, supporting previous phenotypic observations (8). Interestingly, there are strong associations among wild-type *ABCC11*, earwax type (4), axillary osmidrosis

(5, 9, 10), and apocrine colostrum secretion from the mammary gland (11). Furthermore, *ABCC11* mRNA is highly expressed in breast tumours (6, 12, 13).

At the present time, it is not well understood whether wild-type *ABCC11* actually influences breast cancer risk. The present study therefore genotyped the 538G>A SNP in 543 Japanese women to examine the association between the frequency rate of breast cancer and the allele frequency of the wild-type. For this purpose, the SmartAmp method was used to measure 538G>A SNP frequency in *ABCC11* (14, 15). The results suggest that the wild-type allele in *ABCC11* is associated with breast cancer risk.

Patients and Methods

Collection of blood samples from breast cancer patients and control volunteers. Blood samples from 270 Japanese female patients with invasive breast cancer who had been diagnosed at Yokohama City University Medical Centre from 1991 to 2008. In addition, blood samples were also collected from 273 Japanese female volunteers as controls. All blood samples were collected in 2Na-EDTA-coated blood collection tubes. All study participants provided written informed consent and protocols for the present study were approved by the Institutional Review Boards at both Yokohama City University Medical Centre and Mitsui Memorial Hospital. This clinical research study was conducted according to the Declaration of Helsinki Principles. Genotyping of *ABCC11* in the blood samples by the SmartAmp method was approved by the Research Ethical Committee at RIKEN Yokohama Institute.

Clinicopathological data. For breast cancer patients, clinicopathological data was acquired such as age, body mass index (BMI), tumour size, lymph node metastasis (N), the status of the oestrogen receptor (ER), progesterone receptor (PR), and human epidermal growth factor receptor 2 (HER2), triple negative (ER^- PR^- $HER2^-$) tumour phenotype, nuclear grade, and the St. Gallen risk assignment criteria. ER, PR, and HER2 status in breast cancer was determined by immunohistochemistry.

Genotyping of ABCC11 by the SmartAmp method. Detection of the 538G>A SNP in *ABCC11* was performed as described previously (5). Prior to the SmartAmp reaction, the blood samples were incubated at 98°C for 3 min to destroy RNA and to denature proteins and genomic DNA. After chilling on ice, each sample (1 μl) was added directly into the SmartAmp reaction mixture (final total volume of 25 μl). The reaction mixtures were then incubated at 60°C for 40 min under an isothermal condition in a real-time PCR model Mx3000P system (Agilent technologies, La Jolla, CA, USA), where the fluorescence intensity of SYBR® Green I dye indicating DNA amplification was monitored during the reaction.

Statistical rationale. The sample size required for this clinical study was calculated by assuming that 26% of Japanese breast cancer patients and 16% of control volunteers carry G/G homozygote or G/A heterozygote genotypes. The rationale for this assumption originated from Petrakis' pilot study (2), which showed that more Japanese women with breast cancer (9 out of 31; 29%) had the wet type of earwax than did women of the control group (9 out of 52; 17%). The minimum number of subjects needed for confirming significant differences between the cancer and control groups with 80% power was calculated to be 270 in total for a two-sided model at a 5.0% significance level. Thus, for this clinical study, blood samples were collected from a total of 270 Japanese breast cancer patients and 273 Japanese control volunteers.

Statistical analysis. To evaluate the statistical significance of observed data, χ^2 tests were performed using the Dr. SPSS software (SPSS11.5J for Windows; SPSS Inc., Chicago, IL, USA) for univariate analysis and logistic regression for multivariate analyses.

Results

Detection of the 538G>A SNP in ABCC11 by the SmartAmp method. The SmartAmp method can genotype *ABCC11* in blood samples within 40 min (5). Figure 1A depicts the time courses for the SmartAmp reaction that clearly discriminated the three different genotypes (538G/G homozygote, 538G/A heterozygote, and 538A/A homozygote) in human *ABCC11*, where blood samples were pre-treated and incubated as described in the legend of Figure 1A.

The mean age was 52.9±12.52 and 53.3±9.96 years old (mean±S.D.) for the breast cancer patient group and control group, respectively. The mean body mass index (BMI) value was 23.0±3.87 for the breast cancer patient group and 21.0±3.02 for the control group.

Table I compares the *ABCC11* genotypes and earwax type in the study population. The odds ratio was calculated to be 1.63 (p-value=0.026) (Table I).

Figure 1B shows that the relative ratio of breast cancer patients carrying the homozygous 538G/G allele was 1.77-fold greater than that of the corresponding healthy volunteers. This relative ratio was even greater than that (1.41-fold) for breast cancer patients carrying the heterozygous 538G/A allele. The G allele appears to be positively related to breast cancer frequency in the groups of Japanese women studied.

Clinicopathological observations. The prognosis for breast cancer patients with wet earwax has been reported to be worse than for that for patients with dry earwax (2). In this context, it was anticipated in this study that the wet earwax genotypes might have some relation to specific clinicopathological features, such as the status of growth factor receptors or nuclear grade. Since histopathology data were available for all breast cancer patients involved in this clinical study, a possible relationship between *ABCC11* genotypes and clinicopathological features including tumour size, lymph node metastasis, ER, PR, and HER2 status, triple negative tumour phenotype, nuclear grade, tumour stage, and St. Gallen risk was investigated (Table II). Nevertheless, neither chi-square tests nor logistic regression analysis revealed any statistically significant difference between the wet earwax genotypes (538G/G+538G/A) and the dry earwax genotype (538A/A) with respect to the clinicopathological features investigated in this study.

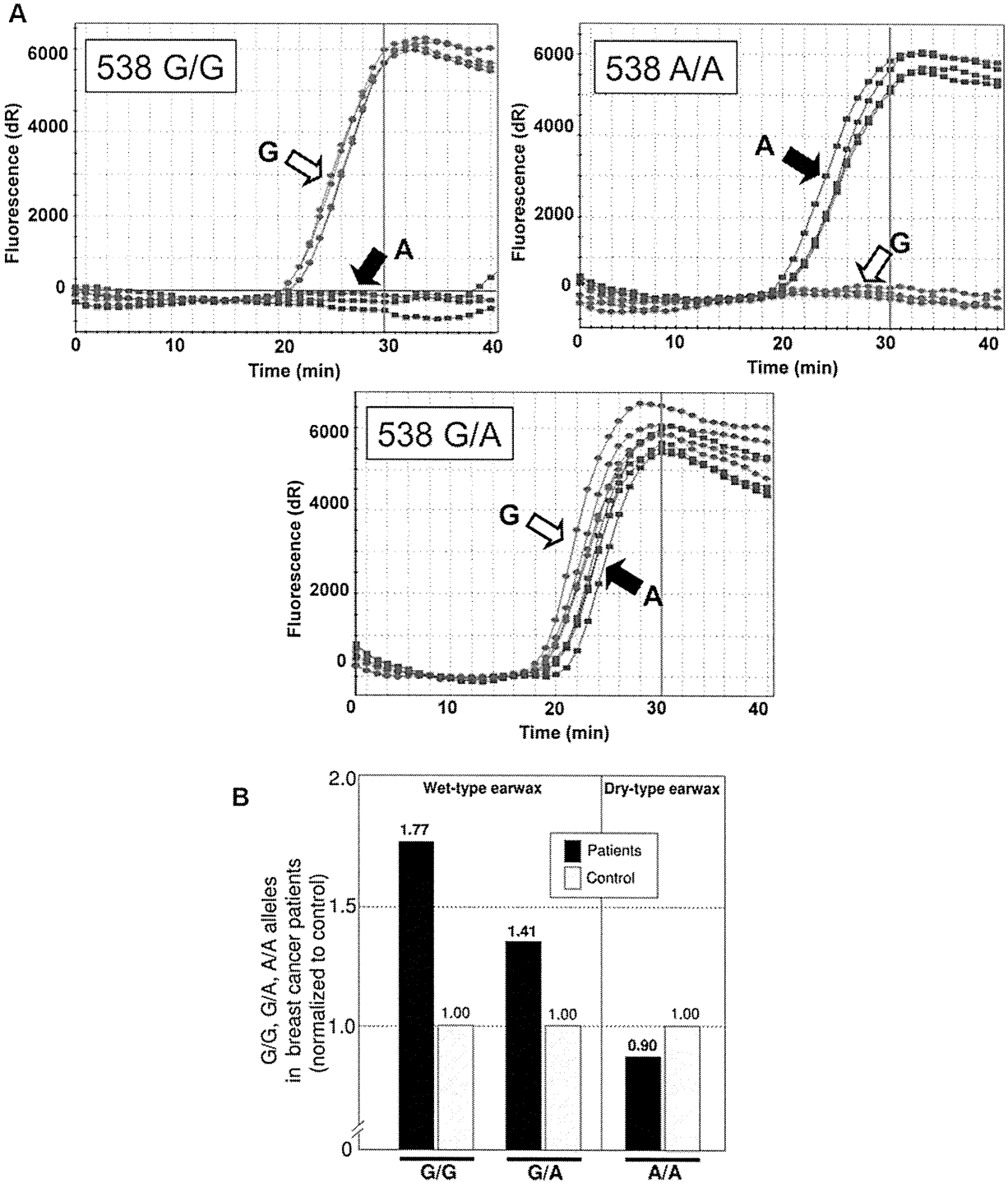

Figure 1. *SmartAmp method-based genotyping of human ABCC11 in blood samples from breast cancer patients and control subjects. A: Blood was mixed with 50 mM NaOH (1:2 v/v) and incubated at 98°C for 3 min. After chilling on ice, 1 μl of the sample was mixed with the SmartAmp reaction mixture (a final total volume of 25 μl) containing 2.0 μM folding primer, 2.0 μM turn-back primer, 1.0 μM boost primer, 0.25 μM of each outer primer, 20 μM competitive probe, 1.4 mM dNTPs, 5% DMSO, 20 mM Tris-HCl (pH 8.0), 10 mM KCl, 10 mM $(NH_4)_2SO_4$, 8 mM $MgSO_4$, 0.1% (v/v) Tween®20, SYBR® Green I (Takara Bio Inc., Shiga, Japan) diluted 1/100,000, and 0.24 unit/μl Aac DNA polymerase (K.K. DNAFORM, Yokohama, Japan). SmartAmp reaction mixtures were incubated at 60°C for 40 min in a real-time PCR model Mx3000P system (Agilent Technologies, La Jolla, CA, USA). The fluorescence intensity of the SYBR® Green I dye was monitored. The time courses represent SmartAmp reactions with ABCC11 allele-specific primers: 538G (red) and 538A (blue). B: Relative ratios of breast cancer patients carrying 538G/G, 538G/A, and 538 A/A alleles. Data are normalised to the controls (female volunteers).*

Table I. *Comparisons of ABCC11 genotypes and earwax type between Japanese breast cancer patients and control subjects.*

	Patients Number (%)	Controls Number (%)	Chi-square test *p*-value
SNP in *ABCC11*			
538G/G	14 (5.19)	8 (2.93)	
538G/A	53 (19.6)	38 (13.9)	
538A/A	203 (75.2)	227 (83.2)	
Phenotype of earwax			
Wet (538G/G + G/A)	67 (24.8)	46 (16.8)	0.026*
Dry (538A/A)	203 (75.2)	227 (83.2)	

*Statistically significant according to the Chi-square tests.

Table II. *Comparison of clinicopathological features between sub-populations with wet-type (538G/G + 538G/A in ABCCC11) and dry-type (538A/A in ABCC11) earwax in Japanese breast cancer patients.*

	538G/G + 538G/A Number (%)	538A/A Number (%)
Tumour size		
<2 cm	32 (51.6)	101 (51.5)
≥2 cm	30 (48.4)	95 (48.5)
Lymph node metastasis		
N (+)	30 (47.6)	81 (40.7)
N (–)	33 (52.4)	118 (59.3)
Receptors		
ER (+)	52 (78.8)	148 (74.0)
ER (–)	14 (21.2)	52 (26.0)
PR (+)	35 (53.8)	116 (58.0)
PR (–)	30 (46.2)	84 (42.0)
HER2 (+)	16 (24.2)	34 (17.3)
HER2 (–)	50 (75.8)	153 (82.7)
Triple negative	5 (7.58)	31 (15.7)
Non-triple negative	61 (92.4)	166 (84.3)
Nuclear grade		
Grade 1 & 2	38 (57.1)	128 (63.4)
Grade 3	21 (35.6)	69 (36.7)
Stage		
1 & 2A	36 (57.1)	128 (63.4)
>2B	27 (42.9)	74 (36.6)
St. Gallen risk		
Low	14 (22.6)	38 (19.3)
Intermediate	30 (49.4)	112 (56.9)
High	18 (29.0)	47 (23.6)

ER: Oestrogen receptor; PR: progesterone receptor. Triple negative means ER (–) PR (–) HER2 (–).

Discussion

Potential role of ABCC11 in breast cancer. The present study provides evidence that the wild type allele of the *ABCC11* gene is associated with breast cancer risk, at least in the Japanese population. About 40 years ago, Petrakis (2) assumed that genetically determined variation in the apocrine system might influence susceptibility to breast cancer, although the genetic determinant (538G>A SNP in *ABCC11*) was not known at that time. It is only recently that more than 10 nonsynonymous SNPs have been found in the human *ABCC11* gene (5, 7). Among those SNPs, one SNP (rs17822931; 538G>A, Gly180Arg) is thought to be a clinically important polymorphism that may related with breast cancer risk.

Genetic polymorphisms of ABCC11 gene. The wild-type (538G or Gly180) human ABC transporter *ABCC11* expressed in apocrine glands plays a pivotal role in earwax secretion (4, 5), axillary osmidrosis (5, 9, 10, 16), and apocrine colostrum secretion from the mammary gland (11). Human ABCC11 reportedly functions as an ATP-dependent efflux pump for amphipathic anions, including oestrone 3-sulfate, dehydroepiandrosterone 3-sulfate (DHEAS), and oestradiol 17-β-D-glucuronide (16-18), suggesting a potential role of ABCC11 in the secretion of steroid metabolites from secretory cells within apocrine glands (16). Indeed, the transport activity of ABCC11 appears to be related to the size of the apocrine glands (5). The genetic polymorphism, on the other hand, has an impact on the *N*-linked glycosylation of ABCC11, intracellular sorting, and proteasomal degradation of the variant protein (5). The SNP variant (538A; Arg180), which lacks *N*-linked glycosylation, is recognised in the endoplasmic reticulum as a misfolded protein that is readily ubiquitinated and proteasomally degraded. Thus, the dry type of earwax was determined to be a Mendelian trait with a recessive phenotype (5). As a consequence, the SNP variant (538A or Arg180) fails to perform its transport function (4, 5), and the apocrine glands that are formed are notably small in size (5). Therefore, it is hypothesised that the function of ABCC11 *per se* or a metabolite transported by ABCC11 may stimulate the proliferation of apocrine gland cells. As far as the cell cycle machinery is operating normally, proliferation of apocrine gland cells should stop at certain levels. However, once somatic mutation has occurred in *BRCA1, BRCA2, p21,* or *p53* gene, deleterious and unregulated proliferation of those cells may start.

It has also been reported that ABCC11 is potentially involved in drug resistance in breast cancer. *ABCC11* mRNA is highly expressed in breast tumours (6, 12, 13), in particular, in invasive ductal adenocarcinomas (https://www.oncomine.org/resource/logn.html). Its expression is reportedly regulated by ER-α (19) and induced by 5-fluorouracil (5-FU) (20). In addition, it has been reported that ABCC11 is directly involved in 5-FU resistance by the efflux transport of the active metabolite 5-fluoro-2'-deoxyuridine 5'-monophosphate (FdUMP) (20-22). It remains to be elucidated, however, whether the expression of

wild-type *ABCC11* (538G) is related to drug resistance in breast cancer and high rates of mortality. In conclusion, the present study shows that Japanese women with wet earwax have a higher relative risk of developing breast cancer than those with dry earwax. Further examination of the *ABCC11* SNPs that determine these phenotypes may provide useful insights into the mechanisms by which breast cancer develops and progresses, including drug resistance and chemosensitivity.

Acknowledgements

The Authors thank Drs. Susan E. Bates and Stephen J. Chanock (National Cancer Institute, NIH) for their helpful discussions. This study was supported by a Research Grant for RIKEN Omics Science Centre from the Ministry of Education, Culture, Sports, Science, and Technology (MEXT) and the Japan Science and Technology Agency (JST) research project named, 'Development of the World's Fastest SNP Detection System.' Yu Toyoda is a research fellow of Japanese Society for the Promotion of Science (JSPS).

References

1 Gaudet MM, Milne RL, Cox A, Camp NJ, Goode EL, Humphreys MK, Dunning AM, Morrison J, Giles GG, Severi G, Baglietto L, English DR, Couch FJ, Olson JE, Wang X, Chang-Claude J, Flesch-Janys D, Abbas S, Salazar R, Mannermaa A, Kataja V, Kosma VM, Lindblom A, Margolin S, Heikkinen T, Kämpjärvi K, Aaltonen K, Nevanlinna H, Bogdanova N, Coinac I, Schürmann P, Dörk T, Bartram CR, Schmutzler RK, Tchatchou S, Burwinkel B, Brauch H, Torres D, Hamann U, Justenhoven C, Ribas G, Arias JI, Benitez J, Bojesen SE, Nordestgaard BG, Flyger HL, Peto J, Fletcher O, Johnson N, Dos Santos Silva I, Fasching PA, Beckmann MW, Strick R, Ekici AB, Broeks A, Schmidt MK, van Leeuwen FE, Van't Veer LJ, Southey MC, Hopper JL, Apicella C, Haiman CA, Henderson BE, Le Marchand L, Kolonel LN, Kristensen V, Grenaker Alnaes G, Hunter DJ, Kraft P, Cox DG, Hankinson SE, Seynaeve C, Vreeswijk MP, Tollenaar RA, Devilee P, Chanock S, Lissowska J, Brinton L, Peplonska B, Czene K, Hall P, Li Y, Liu J, Balasubramanian S, Rafii S, Reed MW, Pooley KA, Conroy D, Baynes C, Kang D, Yoo KY, Noh DY, Ahn SH, Shen CY, Wang HC, Yu JC, Wu PE, Anton-Culver H, Ziogoas A, Egan K, Newcomb P, Titus-Ernstoff L, Trentham Dietz A, Sigurdson AJ, Alexander BH, Bhatti P, Allen-Brady K, Cannon-Albright LA, and Wong J; Australian Ovarian Cancer Study Group and Chenevix-Trench G, Spurdle AB, Beesley J, Pharoah PD, Easton DF and Garcia-Closas M: Breast Cancer Association Consortium: Five polymorphisms and breast cancer risk: results from the Breast Cancer Association Consortium. Cancer Epidemiol Biomarkers Prev *18*: 1610-1616, 2009.

2 Petrakis NL: Cerumen genetics and human breast cancer. Science *173*: 347-349, 1971.

3 Ing R, Petrakis L and Ho HC: Evidence against association between wet cerumen and breast cancer. Lancet *1*: 41, 1973.

4 Yoshiura K, Kinoshita A, Ishida T, Ninokata A, Ishikawa T, Kaname T, Bannai M, Tokunaga K, Sonoda S, Komaki R, Ihara M, Saenko VA, Alipov GK, Sekine I, Komatsu K, Takahashi H, Nakashima M, Sosonkina N, Mapendano CK, Ghadami M, Nomura M, Liang DS, Miwa N, Kim DK, Garidkhuu A, Natsume N, Ohta T, Tomita H, Kaneko A, Kikuchi M, Russomando G, Hirayama K, Ishibashi M, Takahashi A, Saitou N, Murray JC, Saito S, Nakamura Y and Niikawa N: A SNP in the *ABCC11* gene is the determinant of human earwax type. Nat Genet *38*: 324-330, 2006.

5 Toyoda Y, Sakurai A, Mitani Y, Nakashima M, Yoshiura K, Nakagawa H, Sakai Y, Ota I, Lezhava A, Hayashizaki Y, Niikawa N and Ishikawa T: Earwax, osmidrosis, and breast cancer: why does one SNP (538G>A) in the human ABC transporter *ABCC11* gene determine earwax type? FASEB J *23*: 2001-2013, 2009.

6 Yabuuchi H, Shimizu H, Takayanagi S and Ishikawa T: Multiple splicing variants of two new human ATP-binding cassette transporters, *ABCC11* and *ABCC12*. Biochem Biophys Res Commun *288*: 933-939, 2001.

7 Toyoda Y, Hagiya Y, Adachi T, Hoshijima K, Kuo MT and Ishikawa T: MRP class of human ABC transporters: Historical background and new research directions. Xenobiotica *38*: 833-862, 2008.

8 Matsunaga E: The dimorphism in human normal cerumen. Ann Hum Genet *25*: 273-286, 1962.

9 Nakano M, Miwa N, Hirano A, Yoshiura K and Niikawa N: A strong association of axillaryosmidrosis with the wet earwax type determined by genotyping of the *ABCC11* gene. BMC Genet *10*: 42, 2009.

10 Inone Y, Mosi T, Toyada Y, Sakurai A, Ishikawa T, Mitani Y, Hayashizaki Y, Yoshimura Y, Kurahashi H and Sakai Y: Correlation of axillary osmidrosis to a SNP in the *ABCC11* gene determined by the Smart Amplification Process (SmartAmp) method. J Plast Reconstr Aesthet Surg *63*: 1369-1374, 2010.

11 Miura K, Yoshiura K, Miura S, Shimada T, Yamasaki K, Yoshida A, Nakayama D, Shibata Y, Niikawa N and Masuzaki H: A strong association between human earwax-type and apocrine colostrum secretion from the mammary gland. Hum Genet *121*: 631-633, 2007.

12 Bera TK, Lee S, Salvatore G, Lee B and Pastan I: MRP8, a new member of ABC transporter superfamily, identified by EST database mining and gene prediction program, is highly expressed in breast cancer. Mol Medicine *7*: 509-516, 2001.

13 Bieche I, Girault I, Urbain E, Tozlu S and Lidereau R: Relationship between intratumoral expression of genes coding for xenobiotic-metabolizing enzymes and benefit from adjuvant tamoxifen in estrogen receptor alpha-positive postmenopausal breast carcinoma. Breast Cancer Res *6*: R252-R253, 2004.

14 Mitani Y, Lezhava A, Kawai Y, Kikuchi T, Oguchi-Katayama A, Kogo Y, Itoh M, Miyagi T, Takakura H, Hoshi K, Kato C, Arakawa T, Shibata K, Fukui K, Masui R, Kuramitsu S, Kiyotani K, Chalk A, Tsunekawa K, Murakami M, Kamataki T, Oka T, Shimada H, Cizdziel PE and Hayashizaki Y: Rapid SNP diagnostics using asymmetric isothermal amplification and a new mismatch-suppression technology. Nat Methods *4*: 257-262, 2007.

15 Aw W, Ota I, Toyoda Y, Lezhava A, Sakai Y, Gomi T, Hayashizaki Y and Ishikawa T: Pharmacogenomics of human ABC transporters: detection of clinically important SNPs by SmartAmp2 method. Curr Pharm Biotech *12*: in press, 2011.

16 Martin A, Saathoff M, Kuhn F, Max H, Terstegen L and Natsch A: A functional *ABCC11* allele is essential in the biochemical formation of human axillary odor. J Invest Dermatol *130*: 529-540, 2009.

17 Chen ZS, Guo Y, Belinsky MG, Kotova E and Kruh GD: Transport of bile acids, sulfated steroids, estradiol 17-beta-D-glucuronide, and leukotriene C4 by human multidrug resistance protein 8 (ABCC11). Mol Pharmacol *67*: 545-557, 2005.

18 Bortfeld M, Rius M, König J, Herold-Mende C, Nies AT and Keppler D: Human multidrug resistance protein 8 (MRP8/ABCC11), an apical efflux pump for steroid sulfates, is an axonal protein of the CNS and peripheral nervous system. Neuroscience *137*: 1247-1257, 2006.

19 Honorat M, Mesnier A, Vendrell J, Guitton J, Bieche I, Lidereau R, Kruh GD, Dumontet C, Cohen P and Payen L: ABCC11 expression is regulated by estrogen in MCF7 cells, correlated with estrogen receptor alpha expression in postmenopausal breast tumors and overexpressed in tamoxifen-resistant breast cancer cells. Endocr Relat Cancer *15*: 125-138, 2008.

20 Oguri T, Bessho Y, Achiwa H, Ozasa H, Maeno K, Maeda H, Sato S and Ueda R: MRP8/ABCC11 directly confers resistance to 5-fluorouracil. Mol Cancer Ther *6*: 122-127, 2007.

21 Guo Y, Kotova E, Chen ZS, Lee K, Hopper-Borge E, Belinsky MG and Kruh GD: MRP8, ATP-binding cassette C11 (ABCC11), is a cyclic nucleotide efflux pump and a resistance factor for fluoropyrimidines 2',3'-dideoxycytidine and 9'-(2'-phosphonylmethoxyethyl)adenine. J Biol Chem *278*: 29509-29514, 2003.

22 Kruh GD, Guo Y, Hopper-Borge E, Belinsky MG and Chen ZS: ABCC10, ABCC11, and ABCC12. Pflugers Arch *453*: 675-684, 2007.

Received September 20, 2010
Revised October 24, 2010
Accepted October 27, 2010

Please cite this article in press as: Okada et al., *SMOC1* Is Essential for Ocular and Limb Development in Humans and Mice, The American Journal of Human Genetics (2011), doi:10.1016/j.ajhg.2010.11.012

ARTICLE

SMOC1 Is Essential for Ocular and Limb Development in Humans and Mice

Ippei Okada,[1,14] Haruka Hamanoue,[1,2,14] Koji Terada,[3] Takaya Tohma,[4] Andre Megarbane,[5] Eliane Chouery,[5] Joelle Abou-Ghoch,[5] Nadine Jalkh,[5] Ozgur Cogulu,[6] Ferda Ozkinay,[6] Kyoji Horie,[7] Junji Takeda,[7,8] Tatsuya Furuichi,[9,10] Shiro Ikegawa,[9] Kiyomi Nishiyama,[1] Satoko Miyatake,[1] Akira Nishimura,[1] Takeshi Mizuguchi,[1,15] Norio Niikawa,[11,12] Fumiki Hirahara,[2] Tadashi Kaname,[13] Koh-ichiro Yoshiura,[12] Yoshinori Tsurusaki,[1] Hiroshi Doi,[1] Noriko Miyake,[1] Takahisa Furukawa,[3] Naomichi Matsumoto,[1,*] and Hirotomo Saitsu[1,*]

Microphthalmia with limb anomalies (MLA) is a rare autosomal-recessive disorder, presenting with anophthalmia or microphthalmia and hand and/or foot malformation. We mapped the MLA locus to 14q24 and successfully identified three homozygous (one nonsense and two splice site) mutations in the SPARC (secreted protein acidic and rich in cysteine)-related modular calcium binding 1 (*SMOC1*) in three families. *Smoc1* is expressed in the developing optic stalk, ventral optic cup, and limbs of mouse embryos. *Smoc1* null mice recapitulated MLA phenotypes, including aplasia or hypoplasia of optic nerves, hypoplastic fibula and bowed tibia, and syndactyly in limbs. A thinned and irregular ganglion cell layer and atrophy of the anteroventral part of the retina were also observed. Soft tissue syndactyly, resulting from inhibited apoptosis, was related to disturbed expression of genes involved in BMP signaling in the interdigital mesenchyme. Our findings indicate that SMOC1/Smoc1 is essential for ocular and limb development in both humans and mice.

Introduction

Microphthalmia with limb anomalies (MLA [MIM 206920]), also known as Waardenburg anophthalmia syndrome or ophthalmoacromelic syndrome, is a rare autosomal-recessive disorder first described by Waardenburg.[1] It is characterized by ocular anomalies ranging from mild microphthalmia to true anophthalmia and by limb anomalies such as oligodactyly, syndactyly, and synostosis of the 4th and 5th metacarpals.[2–4] The genetic cause for MLA has remained unknown.

It is widely known that secreted signaling molecules such as Sonic hedgehog (Shh), wingless-type MMTV integration site family (Wnt), transforming growth factor β (Tgf-β), bone morphogenetic proteins (Bmps), and fibroblast growth factor (Fgf) are involved in the development of many organs and tissues, including the eyes and limbs.[5,6] In particular, mutations in *BMP4* (MIM 112262) have resulted in anophthalmia with systemic manifestations, including polydactyly and/or syndactyly (also known as micropthalmia, syndromic 6, MCOPS6 [MIM 607932]),[7] highlighting importance of BMP signaling in both the developing eye and limb.

SMOC1 (MIM 608488), which encodes SPARC (secreted protein acidic and rich in cysteine)-related modular calcium binding 1, is a member of the SPARC (also known as BM-40) matricellular protein family that modulates cell-matrix interaction by binding to many cell-surface receptors, the extracellular matrix, growth factors, and cytokines.[8,9] SMOCs are extracellular glycoproteins with five domains: an N-terminal follistatin-like (FS) domain, two thyroglobulin-like (TY) domains, a domain unique to SMOC, and an extracellular calcium-binding (EC) domain.[9] SMOC1 is widely expressed in various tissues with localization to basement membranes.[9,10] Although the biological function of SMOC1 remains largely unknown, it has been recently reported that *Xenopus* smoc protein, the ortholog of human SMOC1, acts as a BMP antagonist,[11] suggesting that human SMOC1 can also modulate BMP signaling.

Here, we demonstrate that *SMOC1* mutations cause MLA. We also show that *Smoc1* null mice recapitulated

[1]Department of Human Genetics, Yokohama City University Graduate School of Medicine, 3-9 Fukuura, Kanazawa-ku, Yokohama 236-0004, Japan; [2]Department of Obstetrics and Gynecology, Yokohama City University Graduate School of Medicine, 3-9 Fukuura, Kanazawa-ku, Yokohama 236-0004, Japan; [3]Department of Developmental Biology, Osaka Bioscience Institute, 6-2-4 Furuedai, Suita, Osaka 565-0874, Japan; [4]Division of Pediatrics, Okinawa Prefectural Nanbu Medical Center & Children's Medical Center, 118-1 Ikyoku, Arakawa, Haebaru, Okinawa 901-1193, Japan; [5]Medical Genetics Unit, St. Joseph University, Beirut 1104-2020, Lebanon; [6]Department of Pediatrics, Ege University Faculty of Medicine, 35100 Bornova-Izmir, Turkey; [7]Department of Social and Environmental Medicine, Graduate School of Medicine, Osaka University, 2-2 Yamadaoka, Suita, Osaka 565-0871, Japan; [8]Center for Advanced Science and Innovation, Osaka University, 2-1 Yamadaoka, Suita, Osaka 565-0871, Japan; [9]Laboratory for Bone and Joint Disease, Center for Genomic Medicine, RIKEN, 4-6-1 Shirokanedai, Minato-ku, Tokyo 108-8639, Japan; [10]Laboratory Animal Facility, Research Center for Medical Sciences, Jikei University School of Medicine, 3-25-8, Nishi-Shimbashi, Minato-ku, Tokyo 105-8461, Japan; [11]Research Institute of Personalized Health Sciences, Health Sciences University of Hokkaido, Ishikari-Tobetsu, Hokkaido 061-0293, Japan; [12]Department of Human Genetics, Nagasaki University Graduate School of Biomedical Sciences, Sakamoto 1-12-4, Nagasaki 852-8523, Japan; [13]Department of Medical Genetics, University of the Ryukyus Faculty of Medicine, 207 Uehara, Nishihara, Okinawa 903-0215, Japan
[14]These authors contributed equally to this work
[15]Current address: Laboratory of Biochemistry and Molecular Biology, National Cancer Institute, National Institutes of Health, Building 37, Room 6050, Bethesda, MD 20892, USA
*Correspondence: naomat@yokohama-cu.ac.jp (N.M.), hsaitsu@yokohama-cu.ac.jp (H.S.)
DOI 10.1016/j.ajhg.2010.11.012.

Please cite this article in press as: Okada et al., *SMOC1* Is Essential for Ocular and Limb Development in Humans and Mice, The American Journal of Human Genetics (2011), doi:10.1016/j.ajhg.2010.11.012

MLA phenotypes, indicating that *SMOC1* plays essential roles in both eye and limb development in humans and mice.

Subjects and Methods

Subjects

A total of four families with one or two cases of MLA were analyzed in this study, including three previously reported families (A, B, and C).[12,13] Family X from Turkey, which has been previously described,[14] was newly recruited to this study. Detailed clinical information of all the patients is available in the literature,[12,14] and phenotypes of patients with confirmed mutations are summarized in Table S1 (available online). A total of five affected and 16 unaffected members from the four families were analyzed in the linkage study. Genomic DNA was obtained from peripheral-blood leukocytes with the use of QuickGene 610-L (Fujifilm, Tokyo, Japan) after informed consent had been given. Experimental protocols were approved by the institutional review board of Yokohama City University School of Medicine.

SNP Genotyping, and Fine Mapping with Short Tandem Repeat Markers

Whole-genome SNP genotyping, with the use of GeneChip Human Mapping 50K Array XbaI (Affymetrix, Santa Clara, CA), and fine mapping of possible candidate regions, with the use of additional microsatellite markers, were performed as previously described.[12,15] The list of primers used for fine mapping is presented in Table S2.

Linkage Analysis

Multipoint linkage analyses using aligned SNPs were performed with ALLEGRO software.[16] Two-point linkage analyses of candidate regions were performed with the LINKAGE package MLINK (FASTLINK software, version 5.1). In each program, an autosomal-recessive model of inheritance with complete penetrance and a disease-allele frequency of 0.001 were applied.

Mutation Analysis of Candidate Genes

All coding exons and exon-intron boundaries of *RAD51L1* (MIM 602948), *ACTN1* (MIM 102575), *ERH* (MIM 601191), *SRSF5* (MIM 600914), *DCAF5* (MIM 603812), *COX16*, *EXD2*, *GALNTL1*, *SLC39A9*, *KIAA0247*, *MED6* (MIM 602984), *TTC9* (MIM 610488), *MAP3K9* (MIM 600136), and *SMOC1* (transcript variant 1, GenBank accession number NM_001034852.1) were analyzed in the probands of families A, C, and X. The transcript variant 2 of *SMOC1* (GenBank accession number NM_022137.4) is 3 bp shorter than the variant 1, leading to an in-frame amino acid deletion at position 431. PCR was cycled 35 times at 94°C for 30 s, at 60°C for 30 s, and at 72°C for 30–90 s in a total volume of 20 μl containing 30 ng genomic DNA as a template, 0.5 μM forward and reverse primers, 200 μM each deoxyribonucleotide triphosphate (dNTP), 1 × ExTaq buffer, and 0.25 U ExTaq (Takara). All primers were designed with Primer3 software. Detailed information of primers is available upon request. PCR products were purified with ExoSAP (USB) and sequenced with BigDye Terminator 3.1 (Applied Biosystems) on a 3100 Genetic Analyzer. Sequences of patients were compared to reference genome sequences in the UCSC Genome Browser (February 2009 assembly) with Seqscape software, version 2.1 (Applied Biosystems).

Animals

Smoc1 mutant mice, created with the use of the *Sleeping Beauty* transposon system, have been previously described.[17] Line PV384 was provided by the RIKEN BioResource Center through the National BioResource Project of MEXT, Japan. Three independent mouse lines (no. 1 to no. 3), each with a single insertion in intron 1 of *Smoc1*, were bred as heterozygotes. Lines 1 and 3 were backcrossed for at least four generations to a C57BL/6J background. Line 2 was maintained with a mixed background of C57BL/6J and ICR. We mainly analyzed line 1, but we confirmed similar phenotypes in lines 2 and 3. Animals were housed in accordance with protocols approved by the Institutional Animal Care and Use Committee at Yokohama City University, School of Medicine. PCR genotyping of mice was performed with the use of genomic DNA from yolk-sac, ear, or tail biopsies. The following primers were used: PV384-WF, 5′-AAAGGCTGGGAATTGTTTG A-3′; PV384-WR, 5′-TGCAGCTGAAACTGTCTCTCC-3′; PV384-MF, 5′-TGTCCTAACTGACTTGCCAAA-3′. The PV384-WF/PV384-WR primers amplified a 441 bp wild-type (WT) product, and the PV384-MF/PV384-WR primers amplified a 218 bp mutant product.

Southern Hybridization

Genomic DNA was extracted from livers or tail biopsies of PV384 heterozygous (*Smoc1*$^{Tp/+}$) mice via standard protocols. The gene-trap insertions were analyzed by Southern hybridization with the use of 10 μg of *Sac*I-, *Nde*I-, BglII-, and *Eco*RI-digested DNA. The probe (451 bp), which hybridized to the internal ribosome entry site (IRES) in the gene-trap vector, was synthesized with the DIG PCR Probe Synthesis Kit (Roche) with the use of the following primers: 5′-CTAACGTTACTGGCCGAAGC-3′ and 5′-CCCAGATCAGATCCCATACAA-3′. Hybridization, washing, and detection of probes were performed according to the manufacturer's protocol. Images were captured with the FluorChem system (Alpha Innotech).

Cloning of Gene-Trap Insertion Sites

After identification of aberrant DNA fragments by Southern hybridization, *Nde*I-, *Sac*I-, and *Eco*RI-digested DNA from PV384 mice was fractionated by electrophoresis, and appropriately sized fragments containing *Ol1* (*other locus 1*), *Ol2*, and *Ol3* were isolated with a QIAEXII Gel Extraction Kit (QIAGEN). The isolated DNA was self-ligated by Ligation High ver.2 (Toyobo), precipitated with ethanol, and dissolved in 20 μl EB buffer (QIAGEN). Inverse PCR was performed in 25 μl reactions, containing 2 μl ligated DNA, 1 × PCR buffer for KOD FX, 0.4 mM each dNTP, 0.5 μM each primer, and 0.5 U KOD FX DNA polymerase (Toyobo). Primers common to *Ol1*, *Ol2*, and *Ol3* were as follows: Inv-F, 5′- AT CGCCAGTTCTGTATGAACGGTCTGGTCTT-3′; Inv-R, 5′-CCCTC TTTACGTGCCAGCCATCTTAGAGATAC-3′. Confirmatory PCR of gene-trap insertion sites for *Ol1*, *Ol2*, and *Ol3* loci was performed with the use of the following primers: *Ol1*-F, 5′-GAGTGGTATTCA TTGGATTCTGCTGAT-3′; *Ol2*-F, 5′-AAATCCAGCTGGCCAACAGA CTAAG-3′; *Ol3*-F, 5′-TTGCCGGGTAGACTCTATCAAGAACCA-3′; TBAL-R, 5′-CTTGTGTCATGCACAAAGTAGATGTCC-3′. Primer sets of *Ol1*-F/TBAL-R, *Ol2*-F/TBAL-R, and *Ol3*-F/TBAL-R could amplify 175 bp, 607 bp, and 767 bp products, respectively. These PCR primer pairs were also used for genotyping of mice harboring a single insertion at the *Smoc1* locus.

Please cite this article in press as: Okada et al., *SMOC1* Is Essential for Ocular and Limb Development in Humans and Mice, The American Journal of Human Genetics (2011), doi:10.1016/j.ajhg.2010.11.012

Confirmation of Promoter- and Poly(A)-Trapped Transcripts

Whole embryos at embryonic day 10.5 (E10.5) and E11.5 were stored in RNAlater solution (QIAGEN). Total RNA was extracted from WT, *Smoc1*$^{Tp/+}$, and *Smoc1*$^{Tp/Tp}$ embryos with the use of RNeasy Plus Mini (QIAGEN). One microgram total RNA was subjected to reverse transcription with the use of a PrimeScript 1st Strand Synthesis Kit with random hexamers (Takara). A control reaction with no reverse transcriptase was included in each experiment. PCR was performed in 20 μl reactions, containing 1 μl cDNA, 1 × PCR Buffer for KOD FX, 0.4 mM each dNTP, 0.3 μM each primer, and 0.4 U KOD FX (Toyobo). Primers used are listed below: *Smoc1*-F, 5′-GTCCCCACCTCCCCAAGTGCTTTGA-3′; *LacZ*-R, 5′-TGCCAAAAGACGGCAATATGGTGGAAA-3′; *GFP*-F, 5′-TCACATGGTCCTGCTGGAGTTCGTGAC-3′; *Smoc1*-R, 5′-ACACTTGCTCTGGCCAGCATCTTTGCAT-3′. Primer sets of *Smoc1*-F/*Smoc1*-R, *Smoc1*-F/*LacZ*-R, and *GFP*-F/*Smoc1*-R could amplify native *Smoc1* (366 bp), promoter-trapped transcripts (Tp-LacZ, 500 bp) and poly(A)-trapped transcripts (Tp-GFP, 308 bp), respectively. The PCR conditions were 98°C for 10 s, 68°C for 1 min, for 30 cycles. Primers for *ACTB*[18] were used as an internal control. PCR for *ACTB* was cycled 20 times at 94°C for 20 s, 60°C for 20 s, and 72°C for 30 s in a total volume of 10 μl containing 0.5 μl cDNA, 0.4 μM each primer, 0.2 mM each dNTP, 1 × ExTaq buffer, and 0.5 U ExTaq HS (Takara). All PCR products were electrophoresed on 2% agarose gels.

In Situ Hybridization

Embryos were collected between E9.5 and E13.5. Whole-mount in situ hybridization was carried out as previously described.[19,20] Two fragments of *Smoc1* cDNA were obtained as probes by RT-PCR, with the use of total RNA extracted from livers of E16.5 mouse embryos, and subcloned into pCR4-TOPO (Invitrogen). Primer sequences were as follows: probe 1-F, 5′-GTCTGCTCACGCCCCACT-3′; probe 1-R, 5′-CCTGAACCATGTCTGTGGTG-3′; probe P-F, 5′-CAGGAACAGGAAAGGGAAGA-3′; probe P-R, 5′-AAGGGAAAACCACACAGCAC-3′. PCR products were 1023 bp and 1578 bp, corresponding to nucleotide positions 275–1297 and 1849–3426 of the mouse *Smoc1* cDNA (GenBank accession number NM_001146217.1), respectively. The cDNA fragment amplified with probe P-F and probe P-R primers was identical to the probe used in a previous report.[21] Digoxigenin-labeled sense and antisense riboprobes were synthesized with the use of a digoxigenin RNA labeling kit (Roche). These two different antisense probes demonstrated identical staining patterns, and the control sense probes showed no staining. The expression pattern was confirmed with more than three embryos. In addition, the following probes were used: *Bmp2* (gift from Y. Takahashi),[22] *Sox9* (gift from A. Yamada),[22] *Bmp7* (gift from E.J. Robertson), and *Msx2* (gift from Dr. R.E. Maxson, Jr). The numbers of embryos examined were as follows (numerical quantity for WT, *Smoc1*$^{Tp/+}$, and *Smoc1*$^{Tp/Tp}$, respectively, shown in parentheses): *Msx2* (2, 1, 3) at E11.5; *Bmp2* (3, 0, 3), *Bmp7* (3, 0, 3), *Msx2* (3, 0, 3), and *Sox9* (2, 1, 3) at E12.5; *Bmp2* (1, 2, 3), *Bmp7* (2, 1, 3), *Msx2* (1, 2, 3), and *Sox9* (1, 3, 4) at E13.5. Stained embryos were cleared in glycerol to enable images to be produced with a VHX-1000 digital microscope (Keyence).

Histology

Heads of embryos and newborns were fixed overnight in 4% paraformaldehyde in PBS at 4°C. These embryos were then washed in PBS. Frozen samples were serially sectioned at 16 μm (E14.5) and 20 μm (P0). The numbers of eyes examined (WT, *Smoc1*$^{Tp/+}$, *Smoc1*$^{Tp/Tp}$) were as follows: coronally sectioned at E14.5 (8, 10, 12), coronally sectioned at P0 (8, 10, 6), horizontally sectioned at P0 (2, 2, 4). For evaluation of ventral atrophy of the retina, only the coronally sectioned eyes were used. TB staining was performed according to standard protocols. Forelimbs of mice were fixed in 4% paraformaldehyde in PBS, decalcified in 10% EDTA, and embedded in paraffin. Forelimbs were serially sectioned at 4 μm and stained with hematoxylin and eosin.

Evaluation of Optic Nerve Diameter

The palatine and orbital bones were carefully removed to expose the optic chiasm and optic nerve. During the dissection process, 4% paraformaldehyde in PBS was frequently applied onto the gaps between the bone and optic nerve. Xylene cyanol was applied to enhance the outline of optic nerves at poastnatal day 0 (P0). Photographs of optic nerves were taken with a VHX-1000 digital microscope, and the diameter was measured for right and left optic nerves with the bundled software included with the VHX-1000 instrument.

Skeletal Staining

For skeletal preparations, mice were fixed in 99.5% ethanol after removal of the skin and viscera. Cartilage tissues were stained with 0.015% alcian blue and 20% acetic acid in 75% ethanol for three days at 37°C. After dehydration with 99.5% ethanol for three days, bones were stained with 0.002% alizarin red in 1% KOH. Then skeletons were cleared in 1% KOH for several weeks. For P14 mice, soft tissues were dissolved in 2% KOH before alizarin red staining.

Nile Blue Staining

For the study of apoptosis of hindlimbs at E13.5 and E14.5, Nile blue (NB) staining was performed on the basis of a previously described protocol,[23] except that staining was performed at 37°C (not room temperature). Apoptosis was determined by NB-stained (deceased) cells. After rinsing in Tyrode solution, hindlimbs of control (WT and heterozygous littermates) and homozygous mice were evaluated. Photographs of dorsal aspects were taken with a VHX-1000 digital microscope. Experiments were repeated three times, and reproducible representative results are presented.

Statistical Analysis

Statistical analyses were performed with the use of non-repeated-measures ANOVA followed by Dunnett's post hoc test. The results are given as mean ± standard deviation, and the threshold p value for statistical significance was 0.01.

Results

Identification of Homozygous *SMOC1* Mutations

We have previously mapped the MLA locus to a 422 kb region at 10p11.23 by analyzing three families (one Japanese family [A] and two Lebanese families [B and C]). This region contained only one gene, *MPP7*, in which no mutations were found.[12] After a new Turkish family (X) was added to the analysis, the MLA locus was again searched by homozygosity mapping to the consanguineous families (X, B, and C) and haplotype mapping to family A for detection of compound-heterozygous mutations; however, we could not detect any common regions

among the four families. We then focused on identifying common regions in any three of the four families to allow for locus heterogeneity (Table S3).

A locus at 14q24.1-q24.2, which showed the highest LOD score (3.936) among the candidate regions larger than 2.0 Mb, was highlighted among families A, C, and X. This locus was analyzed with the use of additional microsatellite markers, and a 3.0 Mb region containing 24 genes was identified (Figures 1A and 1B). A total of 14 genes were sequenced, and homozygous mutations were found in *SMOC1*: c.718C>T (p.Gln240X) in family A, c.664+1G>A in family C, and c.378+1G>A in family X (Figures 1C and 1D). All of these homozygous mutations were cosegregated with the disease phenotype, and the parents of the individuals with these mutations were heterozygous carriers (Figure 1C). We could not find any mutations in *SMOC1* in family B, in which MLA is unlinked to the 14q24.1-q24.2 locus. Interestingly, in family A haplotypes of paternal and maternal alleles, each having the same mutation, are completely different (data not shown), suggesting that the same mutation may have occurred in separate events. The c.718C>T mutation was not detected in 289 healthy Japanese controls, including 100 Okinawa islanders. The other two mutations were not detected in ethnically matched controls (54 Lebanese and 99 Turkish subjects, respectively), nor in 289 Japanese controls. The two splice-donor-site mutations (c.664+1G>A and c.378+1G>A) are predicted to abolish a donor site, as predicted by ESEfinder, NetGene2, HSF2.4.1, SpliceView, and BDGP analysis (Table S4). Thus, the three mutations are likely to lead to a loss of functional SMOC1.

Smoc1 Expression in the Developing Eye and Limb in Mice

For the examination of *Smoc1* expression in the developing eye and limb, whole-mount in situ hybridization of mouse embryos was performed. *Smoc1* was expressed in the forebrain, midbrain, hindbrain, pharyngeal arch, somites, and forelimb buds at E9.5 (Figure 2A). At E10.5, *Smoc1* expression was observed in the optic stalk (Figure 2B), and at E11.5, expression was localized to the closure site of the optic cup (Figure 2C). Expression of *Smoc1* in developing limbs between E10.5 and E11.5 was observed in both dorsal and ventral regions, with a broader pattern of expression in dorsal regions, but expression was not detected in the most anterior, posterior, and distal parts of limb buds (Figures 2D and 2E). Expression coinciding with chondrogenic condensation was observed at E12.5 (Figure 2F), and expression then became restricted to future synovial joint regions at E13.5 (Figure 2G). This dynamic expression suggests that *Smoc1* plays a critical role in ocular and limb development.

Ocular and Limb Anomalies in *Smoc1* Null Mice

To investigate the pathological basis of MLA due to the loss of *SMOC1* function, we obtained *Smoc1* mutant mice, PV384.[17] PV384 mice possess gene-trap insertions in the *Smoc1* locus and in three other loci. After PV384 mice were bred with C57BL/6J or ICR mice, we obtained three independent lines (no. 1 to no. 3), each with a sole insertion in intron 1 of *Smoc1* (Figure S1). We mainly analyzed line 1, but we confirmed similar phenotypes in lines 2 and 3. Heterozygous mutant mice ($Smoc1^{Tp/+}$) were healthy and fertile. Homozygous mice ($Smoc1^{TP/TP}$) were null mutants, as they showed no native transcript of *Smoc1* (Figure S1E). Homozygous mice were viable at P0; however, they did not survive beyond the first 3 wks of life (Figure 3B). Their growth was retarded in comparison to WT and heterozygous littermates at P0 and P14 (Figures 3A and 3C). Developmental defects in eyes and optic nerves were evident at E14.5. Homozygous mice had relatively small eyes, and histological examinations revealed aplasia or hypoplasia of optic nerves (in 10 of 12 optic nerves), atrophy of the anteroventral part of the retina (in 11 of 12 eyes), and extension of the retinal pigmented epithelium (RPE) to the optic nerve (in 10 of 12 eyes) (Figures 3D–3I). These abnormalities were also observed at P0 (aplasia or hypoplasia of optic nerves [in 7 of 10 optic nerves], retinal atrophy [in 6 of 6 eyes], and RPE extension [in 3 of 6 eyes with identifiable optic nerves]) (Figures 3J–3M). WT or heterozygous littermates did not show any such abnormalities, except that a few eyes of heterozygous mice showed extension of the RPE at E14.5, but not at P0 (in 2 of 10 and 0 of 12 eyes, respectively). Toluidine blue (TB) staining showed ganglion cell layers that were thinned and irregular to varying degrees in homozygous mice, suggesting a reduced number of retinal ganglion cells (Figures 3J–3K′). Thus, *Smoc1* is required for axon sprouting, elongation, or maintenance of retinal ganglion cells.[24] Hypoplasia of optic nerves was further quantitatively confirmed by macroscopic examination: the average diameter of optic nerves of homozygous mice was significantly smaller than that of WT and heterozygous littermates at P0 and P14 (Figures 3L–3Q). These data clearly demonstrate that loss of *Smoc1* in mice affects development of the body, retina, and optic nerves, in a manner similar to that seen in MLA patients.[3,4]

Newborn homozygous mice could be readily identified by their hindlimb syndactyly and pes valgus, whereas no abnormalities were observed in WT and heterozygous pups (Figure 4 and Table 1). Interestingly, the severity of syndactyly varied between mouse lines: line 1 exclusively showed soft tissue syndactyly, whereas line 2 frequently showed four digits (Figures 4F and 4J). Skeletal preparations with alcian blue and alizarin red revealed that the foot with four digits had four phalanx and five metatarsals with fusion to each other (Figure 4K). Thus the *Smoc1* null mutation resulted in a spectrum of phenotypes, from soft tissue syndactyly to four fused digits, probably due to different genetic backgrounds. Bowed tibiae and hypoplastic fibulae were also consistently observed in homozygous mice (Figures 4H and 4L). The articulation between

Please cite this article in press as: Okada et al., *SMOC1* Is Essential for Ocular and Limb Development in Humans and Mice, The American Journal of Human Genetics (2011), doi:10.1016/j.ajhg.2010.11.012

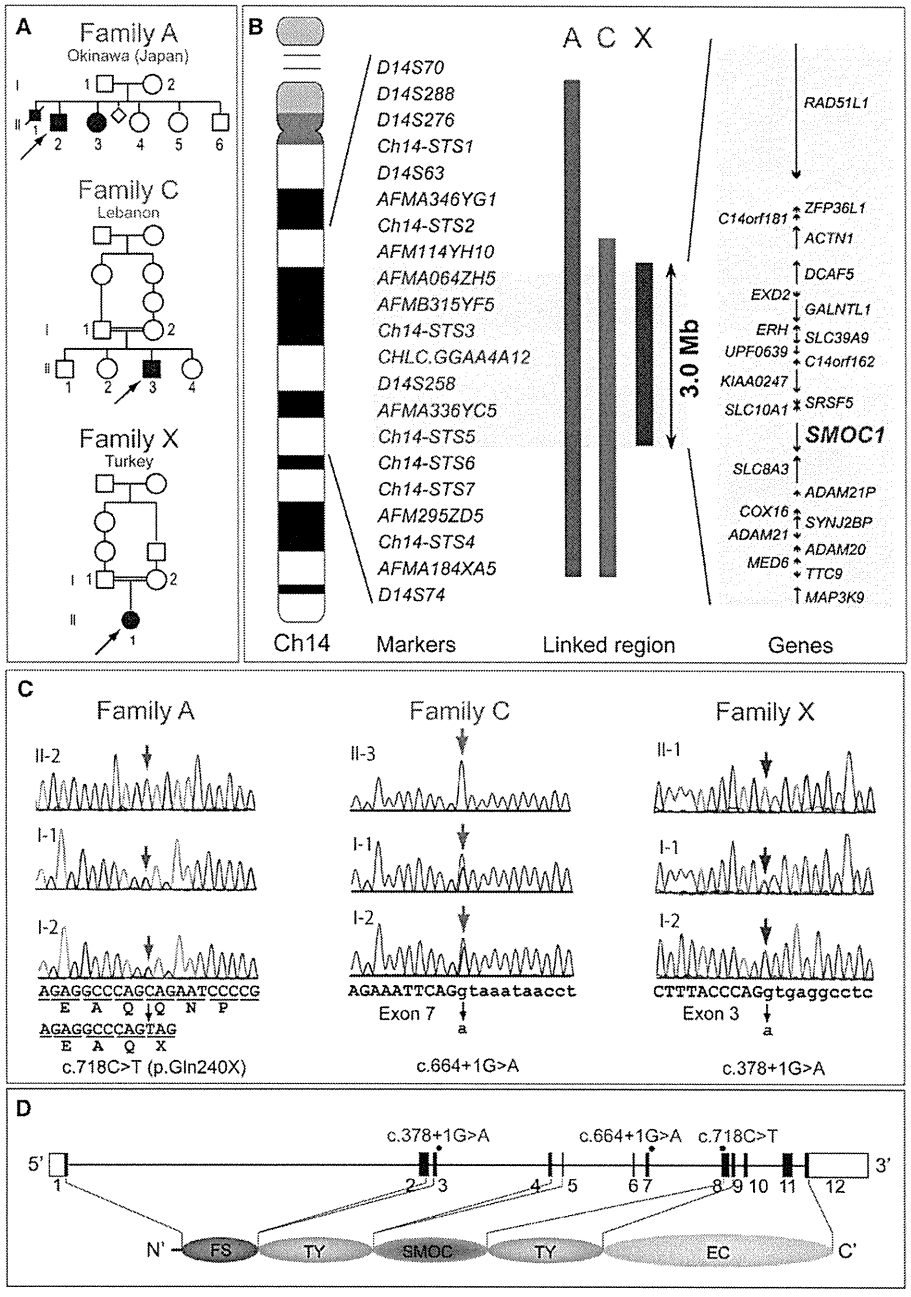

Figure 1. Genetic Analysis of Three Families with Members Affected by Microphthalmia with Limb Anomalies

(A) Pedigrees of the three families.

(B) Linkage analysis with SNPs and microsatellite markers on chromosome 14. From left to right: chromosome ideogram, genetic markers, linked regions of the three families, and genes mapped to the shortest overlapping linked region (between *AFM114YH10* and *Ch14-STS6* [UCSC coordinates, Feb. 2009: chromosome 14: 68,388,190–71,347,908 bp]).

(C) Sequences of mutations identified in each family. Affected patients in family A have a homozygous nonsense mutation (c.718C>T). Patients in families C and X have distinct homozygous splice-donor site mutations (c.664+1G>A and c.378+1G>A, respectively). For all mutations, parents of affected patients are heterozygous carriers, without exception. Sequences of the exon and intron are presented in upper and lower cases, respectively.

(D) At the top is a depiction of a schematic representation of *SMOC1* consisting of 12 exons (UTR and coding exons are indicated by open and filled rectangles, respectively). The locations of three mutations are indicated by red dots. At the bottom, the functional domains of SMOC1 are depicted. Abbreviations are as follows: FS, the follistatin-like domain; TY, the thyroglobulin-like domain; SMOC, the domain unique to SMOC; and EC, the extracellular calcium-binding domain.

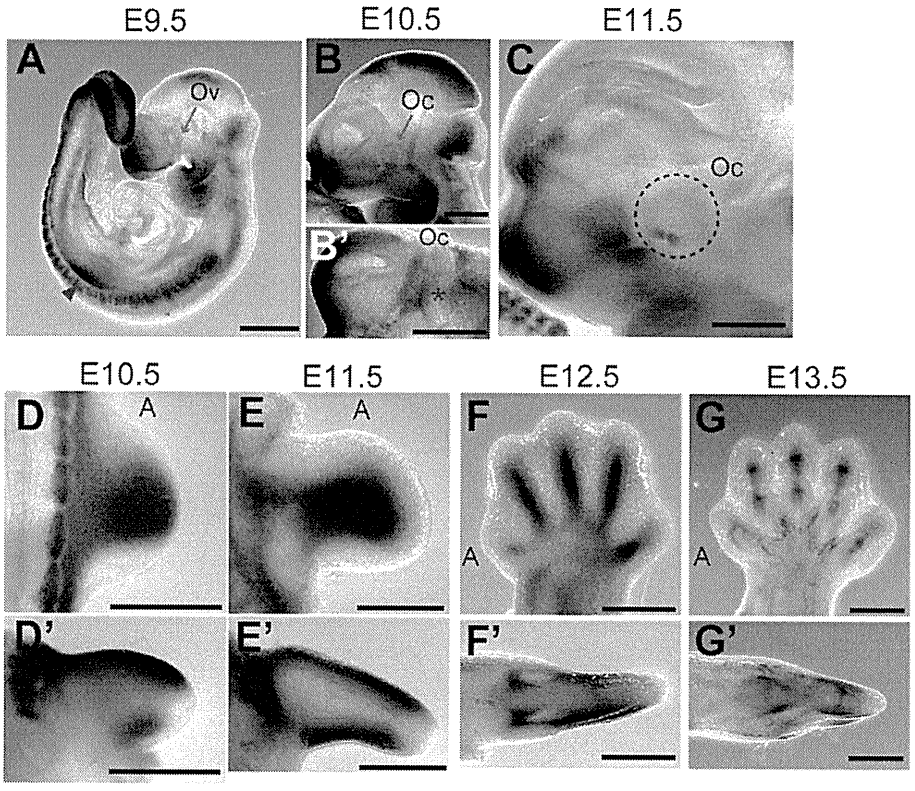

Figure 2. *Smoc1* Expression in Mouse Embryos
Lateral views of embryos (A–C) and a ventral view of the left part of the head (B′, lateral view is shown at the top).
(A) At E9.5, *Smoc1* was expressed in the forebrain, midbrain, hindbrain, pharyngeal arch, somites, and forelimb buds (magenta arrowhead), but not in the optic vesicle (Ov, blue arrow).
(B and B′) Expression in the optic stalk became evident at E10.5 (magenta asterisks), but was not evident in the optic cup (Oc, blue arrow).
(C) Expression was restricted to the closure site of the optic cup (dashed circle) at E11.5.
(D–G) Dorsal and (D′–G′) posterior view of the right hindlimbs (dorsal view is shown at the top in D′–G′). The anterior side is indicated by an A. (D and D′) At E10.5, *Smoc1* was more widely expressed in the dorsal part of the limb bud than in the ventral part. *Smoc1* expression is undetected in the most anterior, posterior, and distal parts of the limb bud. (E and E′) At E11.5, ventral expression was broader than that in the previous stage. (F and F′) At E12.5, expression was detected in areas consistent with chondrogenic condensation. (G and G′) At E13.5, *Smoc1* expression became restricted to future joint regions. Scale bar represents 500 μm.

tibia/fibula and calcanea of homozygous mice appeared malpositioned (Figures 4G and 4K), which might contribute to pes valgus. At P14, soft tissue syndactyly was also evident in most forelimbs of homozygous mice (Figures 4M–4O). Moreover, hindlimbs of homozygous mice showed synostosis between the 4^{th} and 5^{th} metatarsals (Figure 4T), which is observed in both the hands and the feet of MLA patients. Thus, many limb anomalies of MLA patients were recapitulated in *Smoc1* null mice (Table S1).

Reduced Interdigital Apoptosis and Disturbed BMP Signaling

Among the various abnormalities caused by loss of *Smoc1* function, we focused on soft tissue syndactyly, which was commonly observed in both fore- and hindlimbs of null mutants. It is possible that the syndactyly is caused by failed apoptotic regression of the interdigital mesenchyme. To examine this hypothesis, hindlimbs were stained with NB sulfate at E13.5 and E14.5, the time when interdigital apoptosis is most evident. In control embryos (WT and heterozygous littermates), NB-stained apoptotic cells were identified in the interdigital mesenchyme, where regression of the interdigital webbing occurs in the distal region (Figures 5A and 5C). By contrast, the number of apoptotic cells in the mesenchyme between digits 2 and 3 and digits 3 and 4 was dramatically reduced in homozygous mice at E13.5 and E14.5, along with persistent webbing in the distal region (Figures 5B and 5D, magenta asterisk). BMP signaling is involved in apoptosis of the interdigital mesenchyme.[25,26] *Bmp2*, *Bmp7*, and *Msx2*, a direct target of BMP signaling, were strongly expressed in the interdigital mesenchyme of control hindlimbs at both E12.5 and E13.5. However, the expression of these three genes was profoundly reduced and perturbed in hindlimbs of homozygous mice (Figures 5E–5J). These data suggest that inhibition of apoptosis is spatiotemporally correlated to reduced and/or disturbed expression of genes involved in BMP signaling in the interdigital mesenchyme.

Please cite this article in press as: Okada et al., *SMOC1* Is Essential for Ocular and Limb Development in Humans and Mice, The American Journal of Human Genetics (2011), doi:10.1016/j.ajhg.2010.11.012

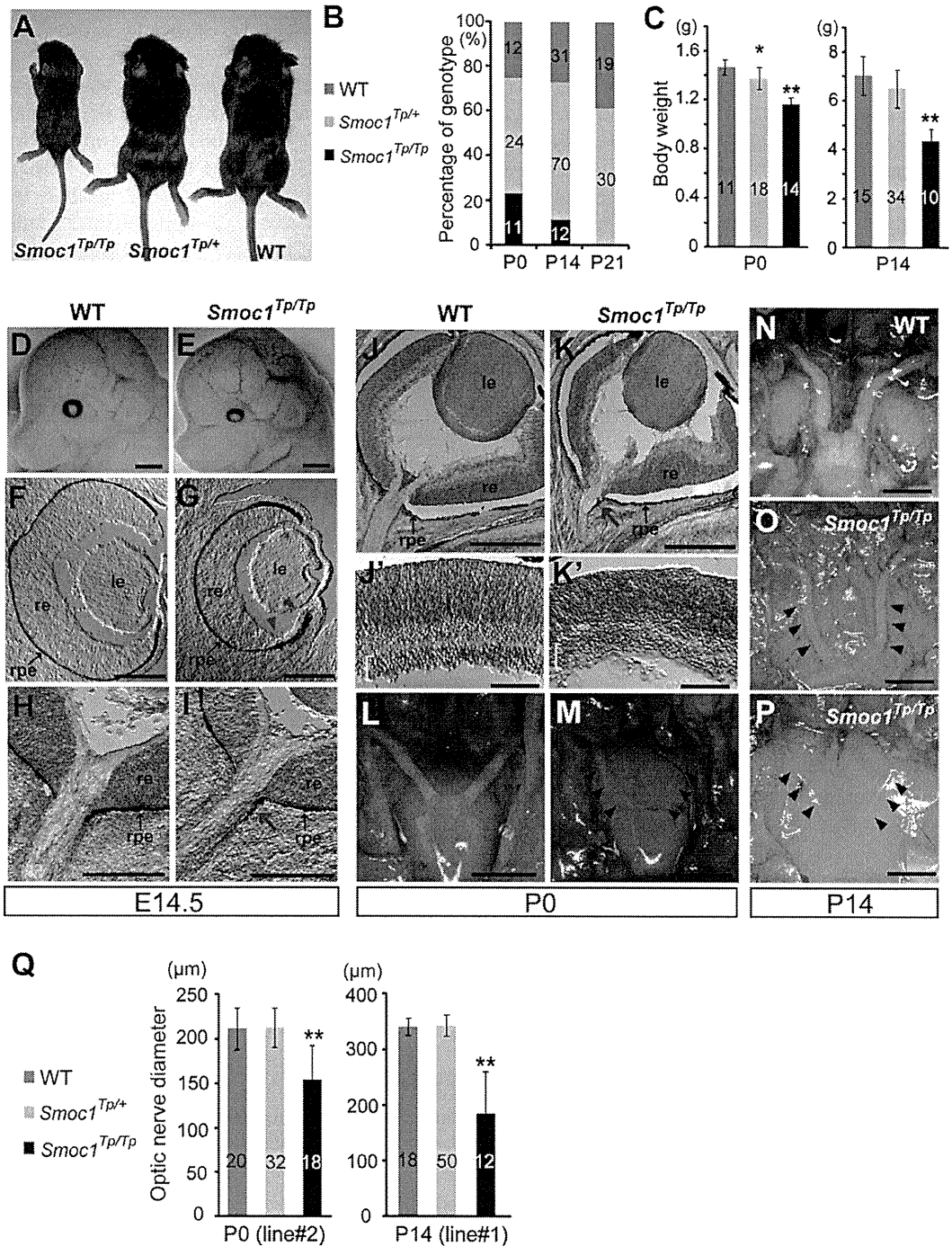

Figure 3. Growth and Ocular Phenotypes of *Smoc1* Null Mice

(A) Representative *Smoc1*$^{Tp/Tp}$ mouse, showing a small body in comparison to *Smoc1*$^{Tp/+}$ and WT littermates.

(B) Genotypes of living pups during the first 3 wk of life.

(C) Body weight of pups of each genotype at P0 (left panel) and P14 (right panel).

(D and E) Relatively small eyes were evident in *Smoc1*$^{Tp/Tp}$ mice in comparison to WT mice.

(F–K′) Coronal sections of eyes at E14.5 (F–I) and P0 (J–K′) with TB staining (H, I, and J–K′). (F-I) Atrophy of the anteroventral part of the retina (G, magenta arrowheads, dorsal view shown at the top), hypoplastic optic nerve, and extension of the RPE to the optic nerve (I, magenta arrow) in *Smoc1*$^{Tp/Tp}$ mice at E14.5. (J and K) Hypoplastic optic nerve and RPE extension in *Smoc1*$^{Tp/Tp}$ mice at P0 (K, magenta arrow). Note that sections in which optic nerves appeared most thick are presented in (H–K). (J′–K′) In higher-magnification views of (J and K), a thinned and irregular ganglion cell layer (white brackets) was observed in *Smoc1*$^{Tp/Tp}$ mice. Abbreviations are as follows: le, lens; re, retina; rpe, retinal pigmented epithelium.

(L–P) Ventral views of the brain showing optic nerves at P0 (L and M) and P14 (N–P), showing various degrees of optic nerve hypoplasia.

Please cite this article in press as: Okada et al., *SMOC1* Is Essential for Ocular and Limb Development in Humans and Mice, The American Journal of Human Genetics (2011), doi:10.1016/j.ajhg.2010.11.012

Discussion

In a previous report, we performed parametric linkage analysis with three families (families A, B, and C) and found 16 loci showing a LOD score ($\theta = 0.000$) higher than 3.0. Additional microsatellite markers highlighted only one locus, 10p11.23.[12] However, no mutations were found in the candidate gene *MPP7*.[12] By recruiting a new family (family X) to this study, we successfully found homozygous mutations in *SMOC1* in families A, C, and X. In family B, no *SMOC1* mutations were found, indicating the genetic heterogeneity in MLA. Patients with *SMOC1* mutations and *Smoc1* null mice showed similar limb anomalies, such as oligodactyly, syndactyly, synostosis of 4th and 5th metacarpals, hypoplasia of fibula, and bowed tibia. Oligodactyly, syndactyly, and synostosis of 4th and 5th metacarpals are common in MLA patients.[2–4] However, hypoplastic fibula and bowed tibia are less common in patients with MLA, as four out of 34 MLA patients showed these anomalies in the previous report.[3] Although one patient with a *SMOC1* mutation from family C did not show bowed tibia and hypoplastic fibula, these anomalies could be features specific to *SMOC1* mutations. Further *SMOC1* analysis of other MLA patients should delineate the phenotypic consequences caused by *SMOC1* mutations.

Accumulating evidence suggests that BMP signaling plays crucial roles in early eye vesicle and limb patterning, skeletal formation, and apoptosis of the interdigital mesenchyme,[25–29] and mutations involving BMP signaling cause human malformations including ocular, limb, and skeletal anomalies.[7,30–33] Here, we present genetic evidence that *SMOC1* is essential for ocular and limb development in humans and mice. Furthermore, *Xenopus smoc* can inhibit BMP signaling,[11] suggesting that *SMOC1/Smoc1* can also modulate BMP signaling in humans and mice. Indeed, we observed reduced and/or disturbed expression of genes involved in BMP signaling in the interdigital mesenchyme in *Smoc1* null mice, and limb and ocular abnormalities associated with loss of *Smoc1* function are consistent with phenotypic consequences of disturbed BMP signaling. Conditional inactivation of *Bmp2* in the limb showed 3/4 syndactyly, and a similar deficiency of both *Bmp2* and *Bmp7* resulted in malformed fibulae in mice.[25] Moreover, mice deficient in *Fmn1*, a repressor of BMP signaling, showed four digits, fused metatarsal bones, and an absence of fibulae in the hindlimbs,[34] suggesting the importance of altered BMP signaling in these features. Concerning ocular phenotypes, haploinsufficiency of mouse *Bmp4* resulted in a decreased number of ganglion layer cells and absence of the optic nerve similar to *Smoc1* null mice,[35] indicating that altered BMP signaling is also involved in the ocular phenotype. Interestingly, knockdown experiments of *smoc* by antisense morpholino in *Xenopus* showed absence or severe deformity of the eye and other anterior structures, which were accompanied by aberrant expression of *otx2*, *tbx2* in the eye field.[11] Mutations of *OTX2* (MIM 600037) cause micropthalmia, syndromic 5 (MCOPS5 [MIM 610125]) in humans.[36] Moreover, targeted disruption of *Tbx2* resulted in a marked reduction in the size of the optic cup and a failure of optic nerve formation in mice.[37] Thus, it is possible that loss of *SMOC1* function could alter the expression of *OTX2* and *TBX2* (MIM 600747) by disturbing BMP signaling in human developing eyes.

It is unknown how the loss of functional SMOC1, a BMP antagonist, leads to reduced expression of genes involved in BMP signaling in the interdigital mesenchyme in *Smoc1* null mice. In the case of *Fmn1*-deficient mice, the loss of the repressor of BMP signaling resulted in downregulation of *Fgf4* and *Shh* and in upregulation of *Gremlin* expression at E10.5, and absence of apoptosis of the interdigital mesenchyme between the two middle digits at E13.5.[34] Thus, there is a possibility that loss of SMOC1 could cause the imbalance among BMP, SHH, and FGF signaling, which would subsequently lead to reduced and/or disturbed expression of genes involved in BMP signaling in the interdigital mesenchyme. In fact, we observed reduced expression of *Msx2* in the progressive zone of hindlimbs at E11.5 (Figure S2). Moreover, expression of *Sox9*, the initial cartilage condensation marker, showed abnormal limb patterning, suggesting that SMOC1 may affect BMP signaling even at early stages of limb development (Figure S3). Further examinations are required for understanding spatial and temporal actions of SMOC1/Smoc1 protein during limb development.

In conclusion, our data demonstrate that *SMOC1/Smoc1* is an essential player in both ocular and limb development in humans and mice and give further support to the crucial roles of BMP signaling in these systems.

Supplemental Data

Supplemental Data include three figures and four tables and can be found with this article online at http://www.cell.com/AJHG/.

Acknowledgments

We would like to thank the patients and their families for their participation in this study. We thank Yoshiko Takahashi (Nara Institute of Science and Technology) and Atsushi Yamada (Showa University) for providing the *Bmp2* and *Sox9* probes; Elizabeth J. Robertson (University of Oxford) and Makoto Ishibashi (Kyoto University) for the *Bmp7* probe; Robert E. Maxson, Jr. (University of Southern California Keck School of Medicine) for the *Msx2*

(Q) Optic nerve diameter. Optic nerves were significantly hypoplastic in $Smoc1^{Tp/Tp}$ mice in comparison to WT and $Smoc1^{Tp/+}$ littermates. The numbers of pups (B and C) or eyes (Q) corresponding to each genotype are indicated within bars. Error bars indicate standard deviation: *$p < 0.01$, compared with WT. **$p < 0.01$, compared with WT and $Smoc1^{Tp/+}$. Scale bars represent 1 mm (D, E, and L–P), 200 μm (F–I), 500 μm (J and K), and 100 μm (J′ and K′).

Please cite this article in press as: Okada et al., *SMOC1* Is Essential for Ocular and Limb Development in Humans and Mice, The American Journal of Human Genetics (2011), doi:10.1016/j.ajhg.2010.11.012

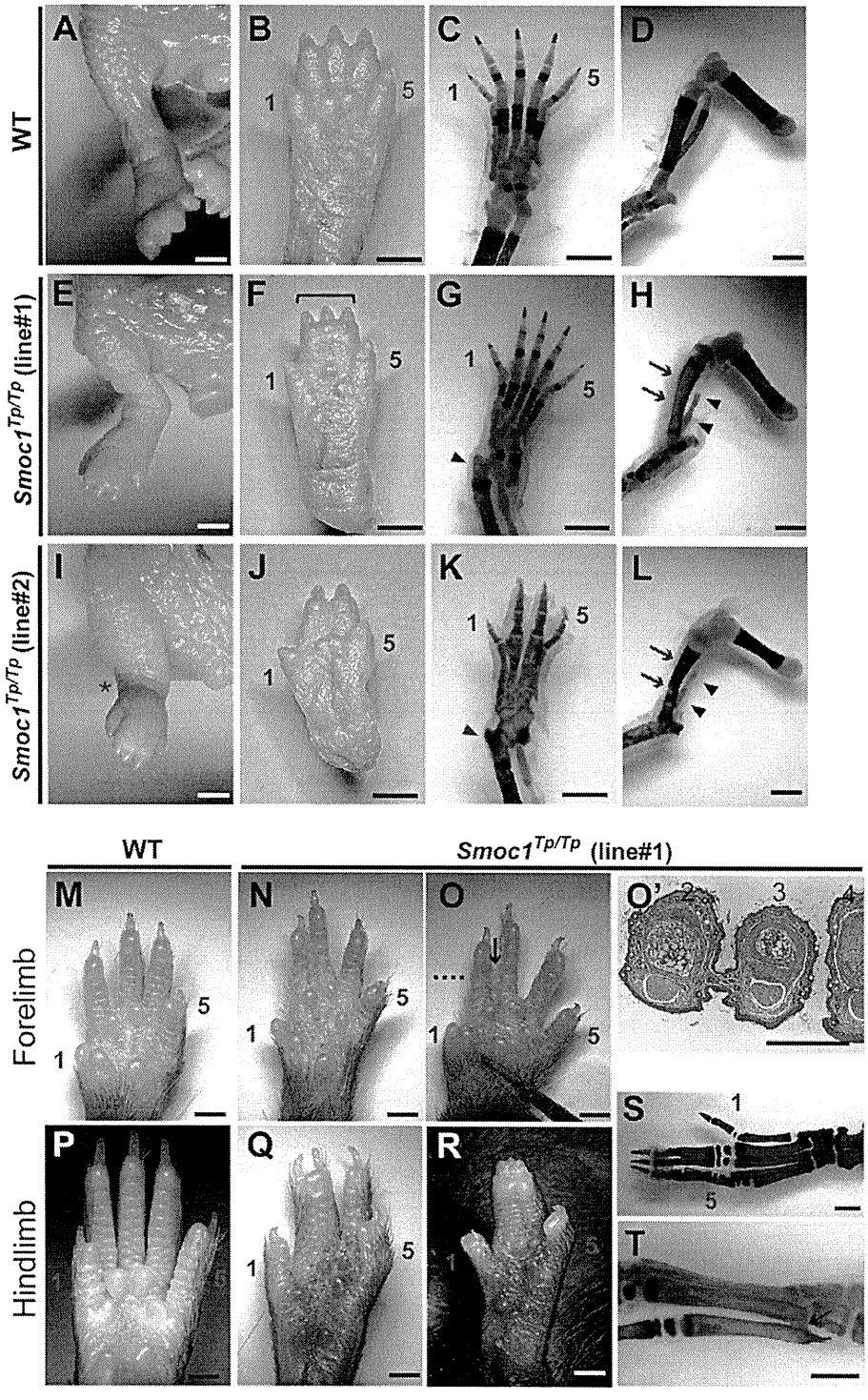

Figure 4. Limb Phenotypes of *Smoc1* Null Mice

Limbs of WT (A–D, M, and P) and *Smoc1*$^{Tp/Tp}$ mice (E–L, N–O′, and Q–T) at P0 (A–L) and P14 (M–T). Digit identities are indicated by the numbers 1 (thumb, anterior) and 5 (little finger, posterior). Skeletal staining with alcian blue and alizarin red is presented (C, D, G, H, K, L, S, and T). *Smoc1*$^{Tp/Tp}$ mice showed pes valgus (E and I), soft tissue syndactyly (F and G), and four digits with metatarsal fusion (J and K). Malposition of the articulation between the tibia/fibula and the calcanea (G and K, magenta arrowheads), bowed tibia (magenta arrows), and hypoplastic fibula (arrowheads) of *Smoc1*$^{Tp/Tp}$ mice (H and L) were observed. 2/3 soft tissue syndactyly (N) and 2/3 webbing (O) were evident in forelimbs of *Smoc1*$^{Tp/Tp}$ mice. (O′) A transverse section taken at the level indicated by the dashed line in (O) showed 2/3 webbing. 2/3 syndactyly (Q), 2/3/4 syndactyly (R), synostosis between the 2nd and 3rd proximal phalanx and metatarsals (S), and synostosis between the 4th and 5th metatarsals (T, arrow), observed in the hindlimbs of *Smoc1*$^{Tp/Tp}$ mice. Scale bars represent 1 mm (A–O and P–T) or 500 μm (O′).

Please cite this article in press as: Okada et al., *SMOC1* Is Essential for Ocular and Limb Development in Humans and Mice, The American Journal of Human Genetics (2011), doi:10.1016/j.ajhg.2010.11.012

Table 1. Limb Abnormalities in *Smoc1*$^{Tp/Tp}$ Mutants

Genotype	Talipes Valgus (No. of Affected/ Total No. of Pups)	Forelimb Abnormalities (No. of Limbs)	Hindlimb Syndactyly (No. of Limbs)					Other External Abnormalities (No. of Pups)	4th and 5th Metatarsal Fusion (No. of Affected/Total No. of Limbs)
			None	2/3[a]	3/4[b]	2/3/4[c]	4 Digits		
Postnatal Day 0									
Smoc1$^{Tp/+}$ (line 1, C57BL/6J)	0/42	0	84	0	0	0	0		
Smoc1$^{Tp/+}$ (line 2, ICR mixed)	0/38	0	76	0	0	0	0		
Smoc1$^{Tp/Tp}$ (line 1, C57BL/6J)	10/10	0	3	0	3	12	2		
Smoc1$^{Tp/Tp}$ (line 2, ICR mixed)	13/17	1[d]	1	1	9	4	19	cleft palate (3)	
Postnatal Day 14									
Smoc1$^{Tp/+}$ (line 1, C57BL/6J)	0/70	0	140	0	0	0	0		
Smoc1$^{Tp/Tp}$ (line 1, C57BL/6J)	11/11	18[e]	2	7	3	8	2	hypoplastic thumbs (5)	9/10[f]

[a] Syndactyly between the 2nd and 3rd digits.
[b] Syndactyly between the 3rd and 4th digits.
[c] Syndactyly between the 2nd, 3rd, and 4th digits.
[d] 2/3 soft tissue syndactyly.
[e] Eleven limbs showed 2/3 webbing, four limbs showed 2/3 soft tissue syndactyly, and one limb showed 3/4 syndactyly.
[f] Based on examination of skeletal preparations.

probe; Tomonori Hirose, Kazunori Akimoto, and Kazunori Sasaki (Yokohama City University) for providing useful information about mouse breeding, taking photos on a stereo microscope, and mRNA quantification; and Kohei Shiota and Sumiko Kimura (Kyoto University) for helpful comments about NB staining and limb anomalies. This work was supported by research grants from the Ministry of Health, Labour and Welfare (T. Furuichi, N. Miyake, N. Matsumoto, and H.S.) and the Japan Science and Technology Agency (N. Matsumoto), a Grant-in-Aid for Scientific Research from the Japan Society for the Promotion of Science (T. Furuichi and N. Matsumoto), and a Grant-in-Aid for Young Scientist from the Japan Society for the Promotion of Science (K.N., H.D., N. Miyake, and H.S.). This work has been carried out at the Advanced Medical Research Center of Yokohama City University.

Received: September 29, 2010
Revised: November 20, 2010
Accepted: November 26, 2010
Published online: December 30, 2010

Web Resources

The URLs for data presented herein are as follows:

BDGP, http://www.fruitfly.org/
ESEfinder 3.0, http://rulai.cshl.edu/cgi-bin/tools/ESE3/esefinder.cgi?process=home
GenBank, http://www.ncbi.nlm.nih.gov/Genbank/
HSF2.4.1, http://www.umd.be/HSF/
NetGene2, http://www.cbs.dtu.dk/services/NetGene2/
Online Mendelian Inheritance in Man, http://www.ncbi.nlm.nih.gov/Omim
UCSC Genome Browser, http://genome.ucsc.edu/cgi-bin/hgGateway
SpliceView, http://zeus2.itb.cnr.it/~webgene/wwwspliceview.html

References

1. Waardenburg, P.J. (1961). Autosomally-recessive anophthalmia with malformations of the hands and feet. In Genetics and Ophthalmology, P.J. Waardenburg, A. Franceschetti, and D. Klein, eds. (Assen, The Netherlands: Royal Van Gorcum), p. 773.
2. Teiber, M.L., Garrido, J.A., and Barreiro, C.Z. (2007). Ophthalmo-acromelic syndrome: report of a case with vertebral anomalies. Am. J. Med. Genet. A. *143A*, 2460–2462.
3. Garavelli, L., Pedori, S., Dal Zotto, R., Franchi, F., Marinelli, M., Croci, G.F., Bellato, S., Ammenti, A., Virdis, R., Banchini, G., and Superti-Furga, A. (2006). Anophthalmos with limb anomalies (Waardenburg opththalmo-acromelic syndrome): report of a new Italian case with renal anomaly and review. Genet. Couns. *17*, 449–455.
4. Tekin, M., Tutar, E., Arsan, S., Atay, G., and Bodurtha, J. (2000). Ophthalmo-acromelic syndrome: report and review. Am. J. Med. Genet. *90*, 150–154.
5. Adler, R., and Canto-Soler, M.V. (2007). Molecular mechanisms of optic vesicle development: complexities, ambiguities and controversies. Dev. Biol. *305*, 1–13.
6. Zeller, R., López-Ríos, J., and Zuniga, A. (2009). Vertebrate limb bud development: moving towards integrative analysis of organogenesis. Nat. Rev. Genet. *10*, 845–858.
7. Bakrania, P., Efthymiou, M., Klein, J.C., Salt, A., Bunyan, D.J., Wyatt, A., Ponting, C.P., Martin, A., Williams, S., Lindley, V., et al. (2008). Mutations in BMP4 cause eye, brain, and digit

Please cite this article in press as: Okada et al., *SMOC1* Is Essential for Ocular and Limb Development in Humans and Mice, The American Journal of Human Genetics (2011), doi:10.1016/j.ajhg.2010.11.012

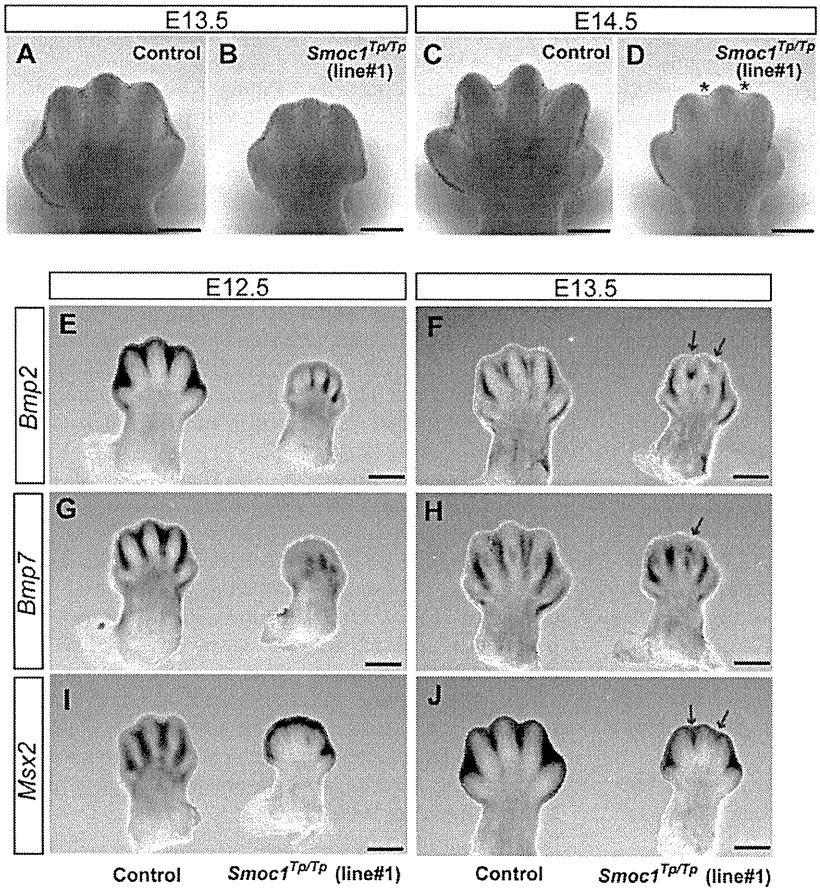

Figure 5. Reduced Apoptosis and Altered BMP Signaling in the Interdigital Mesenchyme of *Smoc1* Null Mice

(A–D) NB staining of left hindlimbs at E13.5 (A and B) and E14.5 (C and D). In comparison to control embryos (WT and $Smoc1^{Tp/+}$ littermates) (A and C), the number of NB-stained apoptotic cells in the interdigital mesenchyme of $Smoc1^{Tp/Tp}$ mice was dramatically reduced between digits 2 and 3 and digits 3 and 4 at both E13.5 and E14.5, and the webbing remained at a distal level (B and D, magenta asterisk).

(E–J) Whole-mount in situ hybridization of right hindlimbs at E12.5 (E, G, and I) and E13.5 (F, H, and J). At E12.5, interdigital expression of *Bmp2*, *Bmp7*, and *Msx2* was profoundly delayed in the hindlimbs of $Smoc1^{Tp/Tp}$ mice, and their expression in the interdigital mesenchyme was apparently perturbed, even at E13.5 (magenta arrows). Scale bar represents 500 μm.

developmental anomalies: overlap between the BMP4 and hedgehog signaling pathways. Am. J. Hum. Genet. *82*, 304–319.

8. Bornstein, P., and Sage, E.H. (2002). Matricellular proteins: extracellular modulators of cell function. Curr. Opin. Cell Biol. *14*, 608–616.
9. Vannahme, C., Smyth, N., Miosge, N., Gösling, S., Frie, C., Paulsson, M., Maurer, P., and Hartmann, U. (2002). Characterization of SMOC-1, a novel modular calcium-binding protein in basement membranes. J. Biol. Chem. *277*, 37977–37986.
10. Gersdorff, N., Müller, M., Schall, A., and Miosge, N. (2006). Secreted modular calcium-binding protein-1 localization during mouse embryogenesis. Histochem. Cell Biol. *126*, 705–712.
11. Thomas, J.T., Canelos, P., Luyten, F.P., and Moos, M., Jr. (2009). Xenopus SMOC-1 inhibits BMP signaling downstream of receptor binding and is essential for post-gastrulation development in Xenopus. J. Biol. Chem. *284*, 18994–19005.
12. Hamanoue, H., Megarbane, A., Tohma, T., Nishimura, A., Mizuguchi, T., Saitsu, H., Sakai, H., Miura, S., Toda, T., Miyake, N., et al. (2009). A locus for ophthalmo-acromelic syndrome mapped to 10p11.23. Am. J. Med. Genet. A. *149A*, 336–342.
13. Mégarbané, A., Souraty, N., and Tamraz, J. (1998). Ophthalmo-acromelic syndrome (Waardenburg) with split hand and polydactyly. Genet. Couns. *9*, 195–199.
14. Cogulu, O., Ozkinay, F., Gündüz, C., Sapmaz, G., and Ozkinay, C. (2000). Waardenburg anophthalmia syndrome: report and review. Am. J. Med. Genet. *90*, 173–174.
15. Miyake, N., Kosho, T., Mizumoto, S., Furuichi, T., Hatamochi, A., Nagashima, Y., Arai, E., Takahashi, K., Kawamura, R., Wakui, K., et al. (2010). Loss-of-function mutations of CHST14 in a new type of Ehlers-Danlos syndrome. Hum. Mutat. *31*, 966–974.
16. Gudbjartsson, D.F., Thorvaldsson, T., Kong, A., Gunnarsson, G., and Ingolfsdottir, A. (2005). Allegro version 2. Nat. Genet. *37*, 1015–1016.
17. Keng, V.W., Yae, K., Hayakawa, T., Mizuno, S., Uno, Y., Yusa, K., Kokubu, C., Kinoshita, T., Akagi, K., Jenkins, N.A., et al. (2005). Region-specific saturation germline mutagenesis in mice using the Sleeping Beauty transposon system. Nat. Methods *2*, 763–769.
18. Mamo, S., Gal, A.B., Bodo, S., and Dinnyes, A. (2007). Quantitative evaluation and selection of reference genes in mouse oocytes and embryos cultured in vivo and in vitro. BMC Dev. Biol. *7*, 14.
19. Parr, B.A., Shea, M.J., Vassileva, G., and McMahon, A.P. (1993). Mouse Wnt genes exhibit discrete domains of expression in the early embryonic CNS and limb buds. Development *119*, 247–261.
20. Saitsu, H., Ishibashi, M., Nakano, H., and Shiota, K. (2003). Spatial and temporal expression of folate-binding protein 1 (Fbp1) is closely associated with anterior neural tube closure in mice. Dev. Dyn. *226*, 112–117.
21. Tamplin, O.J., Kinzel, D., Cox, B.J., Bell, C.E., Rossant, J., and Lickert, H. (2008). Microarray analysis of Foxa2 mutant mouse embryos reveals novel gene expression and inductive roles

for the gastrula organizer and its derivatives. BMC Genomics *9*, 511.

22. Suzuki, D., Yamada, A., Amano, T., Yasuhara, R., Kimura, A., Sakahara, M., Tsumaki, N., Takeda, S., Tamura, M., Nakamura, M., et al. (2009). Essential mesenchymal role of small GTPase Rac1 in interdigital programmed cell death during limb development. Dev. Biol. *335*, 396–406.
23. Kimura, S., and Shiota, K. (1996). Sequential changes of programmed cell death in developing fetal mouse limbs and its possible roles in limb morphogenesis. J. Morphol. *229*, 337–346.
24. Sernagor, E., Eglen, S.J., and Wong, R.O. (2001). Development of retinal ganglion cell structure and function. Prog. Retin. Eye Res. *20*, 139–174.
25. Bandyopadhyay, A., Tsuji, K., Cox, K., Harfe, B.D., Rosen, V., and Tabin, C.J. (2006). Genetic analysis of the roles of BMP2, BMP4, and BMP7 in limb patterning and skeletogenesis. PLoS Genet. *2*, e216.
26. Robert, B. (2007). Bone morphogenetic protein signaling in limb outgrowth and patterning. Dev. Growth Differ. *49*, 455–468.
27. Dudley, A.T., Lyons, K.M., and Robertson, E.J. (1995). A requirement for bone morphogenetic protein-7 during development of the mammalian kidney and eye. Genes Dev. *9*, 2795–2807.
28. Khokha, M.K., Hsu, D., Brunet, L.J., Dionne, M.S., and Harland, R.M. (2003). Gremlin is the BMP antagonist required for maintenance of Shh and Fgf signals during limb patterning. Nat. Genet. *34*, 303–307.
29. Furuta, Y., and Hogan, B.L. (1998). BMP4 is essential for lens induction in the mouse embryo. Genes Dev. *12*, 3764–3775.
30. Asai-Coakwell, M., French, C.R., Berry, K.M., Ye, M., Koss, R., Somerville, M., Mueller, R., van Heyningen, V., Waskiewicz, A.J., and Lehmann, O.J. (2007). GDF6, a novel locus for a spectrum of ocular developmental anomalies. Am. J. Hum. Genet. *80*, 306–315.
31. Tassabehji, M., Fang, Z.M., Hilton, E.N., McGaughran, J., Zhao, Z., de Bock, C.E., Howard, E., Malass, M., Donnai, D., Diwan, A., et al. (2008). Mutations in GDF6 are associated with vertebral segmentation defects in Klippel-Feil syndrome. Hum. Mutat. *29*, 1017–1027.
32. Wyatt, A.W., Osborne, R.J., Stewart, H., and Ragge, N.K. (2010). Bone morphogenetic protein 7 (BMP7) mutations are associated with variable ocular, brain, ear, palate, and skeletal anomalies. Hum. Mutat. *31*, 781–787.
33. Ye, M., Berry-Wynne, K.M., Asai-Coakwell, M., Sundaresan, P., Footz, T., French, C.R., Abitbol, M., Fleisch, V.C., Corbett, N., Allison, W.T., et al. (2010). Mutation of the bone morphogenetic protein GDF3 causes ocular and skeletal anomalies. Hum. Mol. Genet. *19*, 287–298.
34. Zhou, F., Leder, P., Zuniga, A., and Dettenhofer, M. (2009). Formin1 disruption confers oligodactylism and alters Bmp signaling. Hum. Mol. Genet. *18*, 2472–2482.
35. Chang, B., Smith, R.S., Peters, M., Savinova, O.V., Hawes, N.L., Zabaleta, A., Nusinowitz, S., Martin, J.E., Davisson, M.L., Cepko, C.L., et al. (2001). Haploinsufficient Bmp4 ocular phenotypes include anterior segment dysgenesis with elevated intraocular pressure. BMC Genet. *2*, 18.
36. Ragge, N.K., Brown, A.G., Poloschek, C.M., Lorenz, B., Henderson, R.A., Clarke, M.P., Russell-Eggitt, I., Fielder, A., Gerrelli, D., Martinez-Barbera, J.P., et al. (2005). Heterozygous mutations of OTX2 cause severe ocular malformations. Am. J. Hum. Genet. *76*, 1008–1022.
37. Behesti, H., Papaioannou, V.E., and Sowden, J.C. (2009). Loss of Tbx2 delays optic vesicle invagination leading to small optic cups. Dev. Biol. *333*, 360–372.

Journal of Reproductive Immunology 88 (2011) 42–47

Contents lists available at ScienceDirect

Journal of Reproductive Immunology

journal homepage: www.elsevier.com/locate/jreprimm

Coding region polymorphisms in the indoleamine 2,3-dioxygenase (INDO) gene and recurrent spontaneous abortion

Dawar Amani[a,*], Fatemeh Ravangard[a], Norrio Niikawa[b], Ko-ichiro Yoshiura[b], Mojtaba Karimzadeh[c], Alamtaj Samsami Dehaghani[d], Abbas Ghaderi[e,f]

[a] Department of Immunology, Medical School, Ardabil University of Medical Sciences, Ardabil, Iran
[b] Department of Human Genetics, Nagasaki University Graduate School of Biomedical Sciences, 1-12-4 Sakamoto, Nagasaki 852-8523, Japan
[c] Department of Immunology, Medical School, Uromieh University of Medical Sciences, Uromieh, Iran
[d] Department of Obstetrics and Gynecology, Medical School, Shiraz University of Medical Sciences, Shiraz, Iran
[e] Department of Immunology, Medical School, Shiraz University of Medical Sciences, P.O. Box 71345-1798, Shiraz, Iran
[f] Shiraz Institute of Cancer Research, Medical School, Shiraz University of Medical Sciences, P.O. Box 71345-1798, Shiraz, Iran

ARTICLE INFO

Article history:
Received 10 February 2010
Received in revised form 15 July 2010
Accepted 22 July 2010

Keywords:
INDO
Recurrent spontaneous abortion (RSA)
Gene polymorphisms
Iran

ABSTRACT

Indoleamine 2,3-dioxygenase (INDO) catalyzes degradation of the indole ring of indoleamines and locally depletes tryptophan. INDO expression suppresses T cell proliferation and activation. Genetic variation in the INDO gene may contribute to the variable INDO enzyme expression, activity and severity of some diseases. Recurrent spontaneous abortion (RSA) is a common pregnancy complication and the exact causes of RSA are not yet known. We performed an association study between INDO single nucleotide polymorphisms (SNPs) and RSA. To identify INDO SNPs we sequenced DNA samples for ten exons and adjacent intronic regions from 111 RSA patients. Consequently 10 SNPs were detected; four in exons (one in exon 4, two in exon 9 and one in exon 10) and six in intronic regions (one in intron 3, three in intron 6, one in intron 8 and one in intron 9). Three (IVS3+562 del C, IVS8+116 T→ G and IVS9+2431 G→ A) of these ten SNPs have been registered at the NCBI SNP database. Statistical analysis of allele, genotype and haplotype frequency distribution in the three most frequent SNPs (IVS3+562 del C, IVS6+61 G→ A and IVS9+2431 G→ A) showed no significant differences between the 111 RSA and 105 matched control women. CGA and CGG were the most frequent haplotypes in both the RSA and control groups. We conclude that there is no association between INDO polymorphisms and susceptibility of Iranian women to RSA.

1. Introduction

In 1953 Medawar pointed out that survival of the allogenic mammalian conceptus contradicts the laws of tissue transplantation (Medawar, 1953). Since Medawar's publication there have been many discoveries that relate to immune regulation during pregnancy (Billington, 2003). Some of these regulatory mechanisms include: expression of non-polymorphic MHC class I molecules and key roles for cytokines such as IL-10 and TGFβ and Fas ligand (FasL/CD95L). All of these factors contribute to the inhibition of T cell activation at the maternal–fetal interface (Entrican, 2002).

Kamimura et al. (1991) reported a link between indoleamine 2,3-dioxygenase (INDO) expression and pregnancy success in humans. Munn et al. (1998) reported that placental expression of INDO is required to mediate tolerance by maternal CD8+ T cells specific for paternal class I

Abbreviations: INDO, indoleamine 2,3-dioxygenase gene; SNPs, single nucleotide polymorphisms; RSA, recurrent spontaneous abortion.

* Corresponding author. Tel.: +98 9125084787; fax: +98 4515510057.
E-mail address: amanid@sums.ac.ir (D. Amani).

0165-0378/$ – see front matter © 2010 Elsevier Ireland Ltd. All rights reserved.
doi:10.1016/j.jri.2010.07.007